The Canadian Mineralogist
Vol. 44, pp. 45-62 (2006)

ALLANITE-(Ce) IN GRANITIC ROCKS FROM JAPAN: GENETIC IMPLICATIONS OF PATTERNS OF REE AND Mn ENRICHMENT

MIHOKO HOSHINO, MITSUYOSHI KIMATA AND MASAHIRO SHIMIZU

Earth Evolution Sciences, Life and Environmental Sciences,
The University of Tsukuba, Tennodai 1-1-1, Tsukuba, Ibaraki, 305-8572, Japan

NORIMASA NISHIDA

Chemical Analysis Division, Research Facility Center for Science and Technology,
The University of Tsukuba, Tennodai 1-1-1, Tsukuba, Ibaraki, 305-8577, Japan

TAKASHI FUJIWARA

Nippon Chigakukenkyu-kai, Karasuma Demizu, Kamigyo-ku, Kyoto 602-8012, Japan

ABSTRACT

Twenty-two samples of allanite-(Ce) taken from granitic rocks in Japan have been characterized by electron-microprobe analysis. In back-scattered-electron (BSE) images, the allanite-(Ce) is homogeneous or characterized by various types of zoning features: oscillatory, normal or irregular types. Thirteen samples contain appreciable amounts of Mn (0.14–0.59 *apfu*). The Mn-rich crystals (2–6 cm long) are larger than the crystals of Mn-poor allanite-(Ce) (0.5–2 cm long). Samples of the two groups differ considerably from each other in chondrite-normalized REE patterns: Mn-poor allanite-(Ce) is relatively rich in LREE, as is common in igneous allanite, whereas the Mn-rich allanite-(Ce) exhibits an enrichment in the middle rare-earth elements (MREE). The relationship between Mn-rich and Mn-poor allanite-(Ce) is expressed by the coupled substitution Mn^{2+} + (MREE, HREE)$^{3+}$ $\rightleftharpoons$ Ca^{2+} + LREE^{3+}. The presence of Mn-rich allanite-(Ce) in the Japanese island arc, in conjunction with occurrences of Mn-rich and REE-bearing epidote-group minerals in manganese deposits, support a link with subduction-zone processes. The granitic rocks containing Mn-poor allanite-(Ce) belong to the magnetite-series granitic rocks, whereas those containing Mn-rich allanite-(Ce) correspond to the ilmenite series, and seem to have formed from a volatile-enriched magma. Therefore, the Mn content in allanite-(Ce) contains petrogenetic information.

Keywords: allanite-(Ce), rare-earth elements, manganese, chemical zoning, coupled substitution, granitic rocks, origin, crystal size, Japan.

SOMMAIRE

Nous avons caractérisé avec une microsonde électronique la composition chimique de vingt-deux échantillons d'allanite-(Ce) provenant de roches granitiques au Japon. Les images formées par les électrons rétrodiffusés montrent que l'allanite-(Ce) est homogène ou zonée de façon oscillatoire, normale ou irrégulière. Treize échantillons font preuve de quantités importantes de Mn (0.14–0.59 *apfu*). Les cristaux riches en Mn sont plus longs (2–6 cm) que les cristaux à plus faible teneur en Mn (0.5–2 cm). Ces deux groupes d'allanite-(Ce) diffèrent considérablement dans leurs spectres de terres rares normalisés par rapport à une chondrite. L'allanite-(Ce) à faible teneur en Mn est relativement enrichie en terres rares légères (TRL), comme c'est généralement le cas dans l'allanite des roches ignée, tandis que l'allanite-(Ce) riche en Mn montre un enrichissement dans les terres rares moyennes (TRM). La relation entre les deux groupes se décrit par une substitution couplée: Mn^{2+} + (TRM, TR lourdes)$^{3+}$ $\rightleftharpoons$ Ca^{2+} + TRL^{3+}. La présence d'allanite-(Ce) manganifère dans les granites de l'arc insulaire japonais, de même que les indices de minéraux du groupe de l'épidote riches en Mn et en terres rares dans les gisements de manganèse, semblent témoigner d'un lien avec les phénomènes de subduction. Les roches granitiques contenant l'allanite-(Ce) pauvre en Mn font partie de la série de roches granitiques à magnétite, tandis que les roches granitiques contenant l'allanite-(Ce) riche en Mn correspondent à la série à ilménite, et se seraient formées de magmas enrichis en composants volatils. C'est donc dire que la teneur de l'allanite-(Ce) en Mn serait un indicateur de l'origine des roches granitiques.

(Traduit par la Rédaction)

Mots-clés: allanite-(Ce), terres rares, manganèse, zonation chimique, substitution couplée, roches granitiques, origine, taille des cristaux, Japon.

E-mail address: hossy716@arsia.geo.tsukuba.ac.jp

INTRODUCTION

Allanite-(Ce), a member of the epidote group of minerals [$A_2\,M_3\,\mathrm{Si}_3\,\mathrm{O}_{11}\mathrm{O}\,(\mathrm{OH})$, *A*: Ca, Ce; *M*: Al, Fe], is an important host for rare-earth elements (REE), as it occurs as a characteristic accessory mineral in various kinds of rocks: granite, granodiorite, monzonite, syenite, skarns, and felsic volcanic rocks (Deer *et al.* 1986, Gaines *et al.* 1997, Gieré & Sorensen 2004); it also is found in glaucophane schist (Banno 1993). As Ercit (2002) pointed out, there are other species in the allanite subgroup, distinguished on the basis of their REE content: allanite-(La) and allanite-(Y). In most cases, allanite incorporates Th and U. Decay of these elements causes metamictization (Gieré & Sorensen 2004).

In Japan, allanite-(Ce), having an idealized formula $(\mathrm{Ce,Ca,Y})_2(\mathrm{Al,Fe}^{3+})_3(\mathrm{SiO}_4)_3(\mathrm{OH})$, most commonly occurs in granite, granitic pegmatite, gabbroic pegmatite, monzonite pegmatite and granodiorite (Omori & Hasegawa 1956, Nagashima & Nagashima 1960, Hasegawa 1957, 1958, 1959, 1960, 1961), and rarely in metamorphic rocks (Sakai *et al.* 1984, Banno 1993). Until the middle 1990s, the multiplicity of characteristic X-ray lines for REE precluded accurate electron- microprobe analysis (EPMA) of REE-bearing minerals. Development of better methods through careful measurement of these X-ray lines has improved the REE data obtained by EPMA (*e.g.*, Reed & Buckley 1998, Nishida *et al.* 1999). Moreover, back-scattered-electron (BSE) images of allanite grains typically show the presence of zoning controlled by the abundance of light rare-earth elements (LREE), Fe, Th, and U (*e.g.*, Sorensen 1991, Carcangiu *et al.* 1997, Catlos *et al.* 2000). However, almost all chemical compositions of allanite from granitic rocks in Japan were reported prior to the effective use of EPMA. The exception is the allanite from granitic rocks documented by Suzuki *et al.* (1990). Early detailed studies (Hasegawa 1960) confirmed that the Mn content in allanite from Japan are generally higher than those from other countries in the region. High contents of manganese are generally associated with low Ca contents, and the sum of (Mn + Ca) ions is approximately constant in allanite (Deer *et al.* 1986).

TABLE 1. STANDARD MATERIALS USED FOR WAVELENGTH-DISPERSION ELECTRON-MICROPROBE ANALYSIS

Standard	Chemical composition (wt%)			
Y	SiO_2 (54.3)	Al_2O_3 (12.7)	CaO (20.5)	Y_2O_3 (11.8)
La	SiO_2 (54.3)	Al_2O_3 (12.7)	CaO (20.6)	La_2O_3 (11.5)
Ce	SiO_2 (54.2)	Al_2O_3 (12.8)	CaO (20.4)	Ce_2O_3 (11.9)
Pr	SiO_2 (54.0)	Al_2O_3 (12.7)	CaO (20.6)	Pr_2O_3 (12.2)
Nd	SiO_2 (54.4)	Al_2O_3 (12.8)	CaO (20.8)	Nd_2O_3 (11.8)
Sm	SiO_2 (54.8)	Al_2O_3 (12.9)	CaO (20.8)	Sm_2O_3 (11.2)
Gd	SiO_2 (54.8)	Al_2O_3 (12.1)	CaO (20.7)	Gd_2O_3 (12.1)
Tb	SiO_2 (54.6)	Al_2O_3 (12.6)	CaO (20.2)	Tb_2O_3 (11.9)
Dy	SiO_2 (54.7)	Al_2O_3 (12.5)	CaO (20.6)	Dy_2O_3 (12.0)
Er	SiO_2 (54.6)	Al_2O_3 (12.6)	CaO (20.5)	Er_2O_3 (11.9)
Tm	SiO_2 (54.8)	Al_2O_3 (12.4)	CaO (20.3)	Tm_2O_3 (11.9)
Yb	SiO_2 (54.7)	Al_2O_3 (12.6)	CaO (20.7)	Yb_2O_3 (12.0)

All standards are from P & H Development Ltd., U.K.

Our purpose here is document and interpret the chemical compositions of allanite from granitic rocks in Japan and associated with the Japanese island arc in comparison with those from other regions.

ANALYTICAL METHODS

The chemical composition of allanite were determined with a JEOL JXA–8621 electron microprobe equipped with three wavelength-dispersion spectrometers (WDS) at the Chemical Analysis Division, University of Tsukuba. Chemical zoning of allanite was recorded with high resolution using BSE images. Qualitative analyses were made using 25 kV accelerating potential and 2.5×10^{-7} A beam current. New methods of correction for overlap between REE have been developed by Reed & Buckley (1998) and Nishida *et al.* (1999). We adopted the latter method. Quantitative analyses of allanite for major elements were carried out using an accelerating voltage of 25 kV and a beam current 1.0×10^{-8} A. Concentrations of the REE were measured at 25 kV with a beam current 5.0×10^{-8} A. X-ray intensities for Y, La, Ce, Nd, Er, Tb, Tm, Yb were determined using the $L\alpha_1$ X-ray lines, whereas the intensities for Pr, Sm, Gd and Dy peaks were measured using the $L\beta_1$ lines. For REE standards, we used synthetic Ca–Al silicate glasses containing each REE, which are available from P & H Development Ltd. (Table 1). All the data were corrected with a ZAF matrix-correction program. The locations and descriptions of occurrences of the samples analyzed are given in Table 2.

RESULTS

Zoning types and chemical compositions of allanite

Grains of allanite from granitic rocks are known to have three types of optical zoning, as revealed in BSE images: (1) oscillatory zoning (*e.g.*, Deer *et al.* 1986, Buda & Nagy 1995, Dahlquist 2001), (2) normal growth-induced magmatic zoning (Poitrasson 2002, Oberli *et al.* 2004, Gieré & Sorensen 2004), and (3) complicated internal zoning consisting of a patchwork of domains variable in brightness (Petrík *et al.* 1995). However, the chemical zoning for most of the allanite samples presently examined has been defined as of an irregular type (Table 2, Figs. 1b, d, e, f, q, r, s, t, u), although the three types of zoning present (Figs. 1b, s, u) are broadly similar in texture to the complicated pattern of internal zoning (Petrík *et al.* 1995). Under the polarizing microscope, the chemical zones within each of the allanite crystals show simultaneous extinction.

TABLE 2. MINERALOGICAL AND PETROGRAPHIC DATA FOR ALLANITE-(Ce) FROM GRANITIC ROCKS, JAPAN

#	Morphology	Type of zoning	Mn (*apfu*)**	Crystal size (cm)	Host rock***	Series †	Location	Ref. ‡
a	prismatic euhedral	magmatic	0.037-0.043	0.3 × 0.3 × 0.5	GP	magnetite	Miyamori, Iwate	1
b	anhedral	irregular	0.564-0.624	2.5 × 2.5 × 5.0	GP	ilmenite	Suishyoyama, Fukushima	2
c	prismatic euhedral	magmatic	0.054-0.060	0.5 × 0.5 × 1.5	GP	ilmenite	Kitatosawa, Fukushima	2
d	dendritic	irregular	0.099-0.153	-	GP	ilmenite	Shiodaira, Fukushima	1
e	subhedral	irregular	0.215-0.223	0.6 × 0.6 × 2.5	GP	ilmenite	Utsumine, Fukushima	1
f	anhedral	irregular	0.173-0.177	2.0 × 2.0 × 3.5	GP	ilmenite	Matsuzuka, Fukushima	-[§]
g	subhedral	homog.	0.346-0.372	1.0 × 1.5 × 2.0	GP	ilmenite	Shimo-ono, Ibaraki	1
h	subhedral	mixture*	0.525-0.605	1.5 × 1.5 × 4.5	GP	ilmenite	Haguri, Shiga	1
i	prismatic euhedral	oscillatory	0.019-0.070	0.1 × 0.1 × 0.5	G	magnetite	Omiyadani, Shiga	-
j	prismatic euhedral	homog.	0.065-0.079	0.5 × 0.5 × 1.0	GP	magnetite	Daibosatsu, Yamanashi	1
k	anhedral	magmatic	0.040-0.112	0.2 × 0.2 × 0.5	G	magnetite	Nagatejima, Ishikawa	1
l	dendritic	oscillatory	0.049-0.061	-	GP	magnetite	Hirono, Kyoto	-
m	prismatic euhedral	mixture	0.265-0.304	0.5 × 0.5 × 2.0	GP	magnetite	Ōro, Kyoto	1, 3
n	prismatic euhedral	oscillatory	0.014-0.069	0.3 × 0.3 × 1.0	G	magnetite	Daimonjiyama, Kyoto	1
o	anhedral	magmatic	0.157-0.165	3.5 × 3.5 × 4.5	GP	ilmenite	Kamo, Kyoto	-
p	anhedral	magmatic	0.079-0.088	0.5 × 0.5 × 1.5	GP	ilmenite	Daian, Mie	-
q	prismatic euhedral	irregular	0.144-0.168	1.5 × 1.5 × 5.5	GP	ilmenite	Fukudayama, Mie	1
r	anhedral	irregular	0.289-0.364	0.5 × 0.3 × 2.5	GP	ilmenite	Geino, Mie	-
s	anhedral	irregular	0.363-0.455	3.0 × 2.5 × 6.0	GP	ilmenite	Kanayama, Kagawa	4, 5
t	anhedral	irregular	0.307-0.364	3.5 × 3.5 × 5.0	GP	ilmenite	Tateiwa, Ehime	1, 5
u	anhedral	irregular	0.245-0.275	1.0 × 1.0 × 3.0	GP	ilmenite	Tamagawa, Ehime	5
v	subhedral	magmatic	0.112-0.118	0.5 × 0.4 × 2.0	GP	magnetite	Kaho, Fukuoka	-

* Mixture represents a combination of magmatic and irregular types. ** The allanite grains can be divided into Mn-rich type (more than 0.14 *apfu* Mn) and Mn-poor type (less than 0.14 *apfu* Mn). See Table 3-7, Figures 2 and 3. *** Host-rock codes: GP: granitic pegmatite, G: granite. † Granitic rocks are classified according to Ishihara (1977, 1981), Shibata & Ishihara (1979) and Takagi (2004). ‡ Reference for locality: 1 Nagashima & Nagashima (1960), (2) Hasegawa (1957), (3) Yamada *et al.* (1980), (4) Hasegawa (1958), and (5) Hasegawa (1959). -[§]: no reference.

Representative compositions of allanite are provided in Tables 3–7. The EPMA data demonstrate that Ce is predominant over other REE in all allanite grains studied here; they are thus identified as allanite-(Ce). Different degrees of metamictization are exhibited as a result of variability in radionuclide content (particularly Th), as confirmed by X-ray-diffraction patterns. A single smooth hump is produced by diffuse scattering of X rays by the aperiodic material; most of the allanite samples studied are in a slightly metamict or non-metamict state, except for those from Miyanomori, Shimo-ono, Kamo and Fukudayama (Hoshino *et al.* 2005). The WDS analytical results presented here show that Eu is below the detection limit in all samples. Of the 22 samples examined, thirteen contain appreciable amounts of Mn (0.14–0.59 atoms per formula unit, *apfu*). The samples may be divided into Mn-rich (Mn > 0.14 *apfu*) and Mn-poor allanite (Mn < 0.14 *apfu*) (Tables 2–7, Figs. 2, 3). Most of the allanite-(Ce) samples exhibit A-site vacancies to varying degrees (Table 3–7). The mechanism of incorporation of vacancies will be discussed later. Their structural formulae were first calculated by normalizing the ($M + T$) cations to 6 *apfu*; this normalization is followed by varying Fe^{2+}/Fe^{3+} until the total number of positive charges equals 25 (Ercit 2002). The assignment of cations based on charge balance is summarized in Tables 3–7.

The Mn-bearing allanite-(Ce) is crystal-chemically different from androsite, REE-bearing piemontite and khristovite, as clearly distinguished in an $\Sigma REE - (Fe^{2+} + Fe^{3+}) - (Mn^{2+} + Mn^{3+})$ diagram (Fig. 2). Compilation of the present and previous data on allanites from granitic rocks (Fig. 3) shows that a general decrease in Ca can be observed with increasing total Mn. However, a correct understanding of this observation involves the distribution of Mn between the *A* and *M* sites. Therefore, a trace of Mn^{2+} is interpreted to occupy the *M*3 site in our samples. Concerning the other Mn-bearing epidote-group minerals, REE-bearing piemontite shows extensive solid-solution toward allanite (Bonazzi *et al.* 1992, Bonazzi & Menchetti 1994, Bermanec *et al.* 1994) as a result of the coupled substitution $Ca^{2+} + Mn^{3+} \rightleftharpoons REE^{3+} + Fe^{2+}$ (Gieré & Sorensen 2004). On the other hand, khristovite (Sokolova *et al.* 1991) contains Mn^{2+} rather than Mg at the *M*3 site (Gieré & Sorensen 2004). This Mn^{2+} site-preference is consistent with the result obtained from the present analyses.

The chemical zoning observed in the allanite grains seems to be caused by variations in Th, Fe^{2+}, Fe^{3+}, Mn, and REE contents (Tables 3–7). In the BSE images, Mn-poor allanite displays either an almost

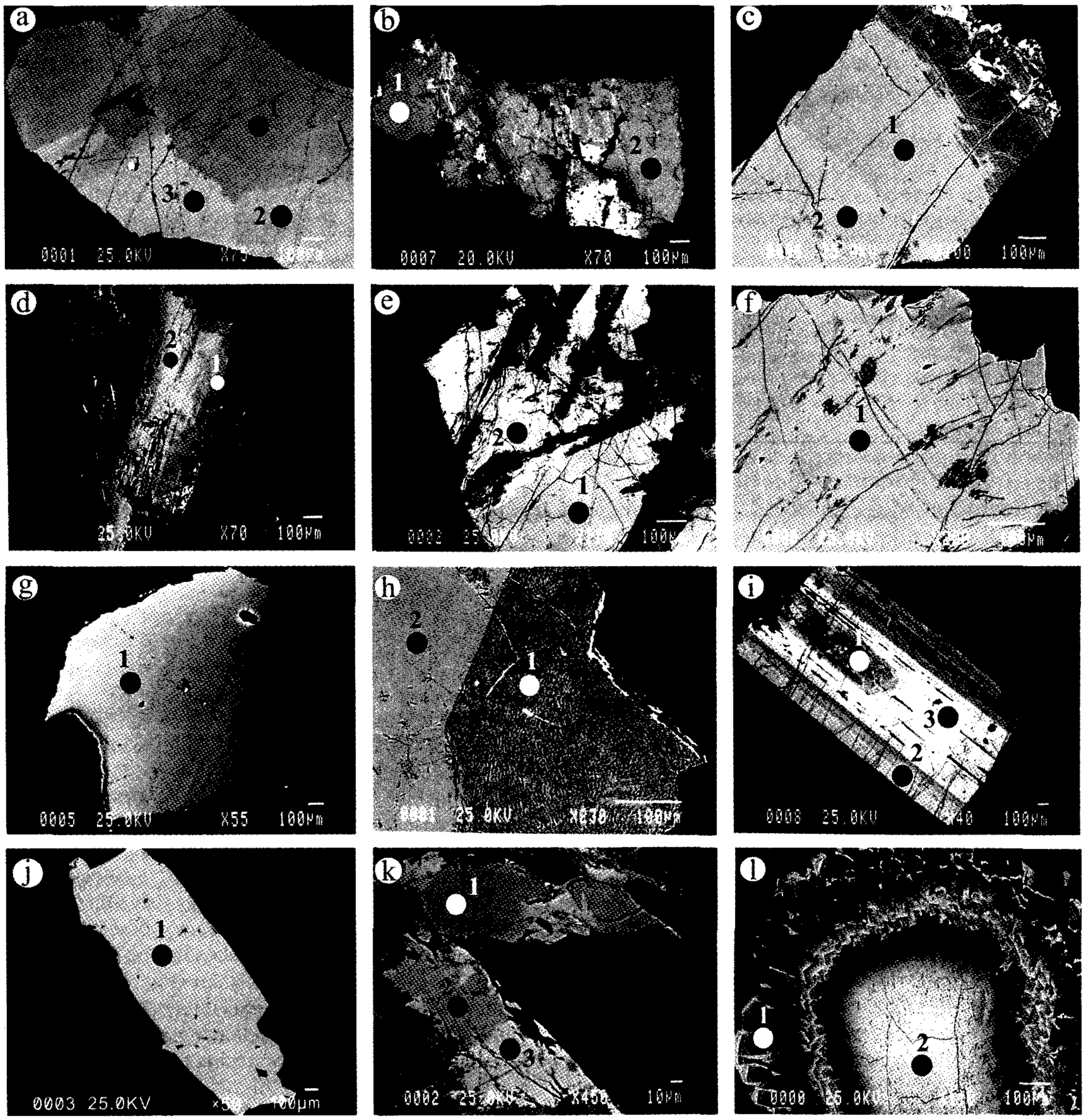

homogeneous distribution of elements or an oscillatory magmatic zoning, whereas most Mn-rich samples exhibit irregular zoning. Moreover, Mn-poor allanite tends to have a euhedral or subhedral shape, in contrast with the Mn-rich grains, which are mostly anhedral crystals (Table 2).

DISCUSSION

A-site vacancies in allanite

Although the *A* sites of some allanties may be partially vacant, it is difficult to document the presence of vacancies due to the chemical complexity of the mineral, and especially the uncertainties of the calculation of Fe^{2+}/Fe^{3+} from electron-microprobe data (Ercit 2002, Gieré & Sorensen 2004). However, corroborative evidence exists to support the idea that vacancies may occur at the *A* site of allanite and related minerals. In conjunction with electron-microprobe data, the structural refinement of khristovite-(Ce) yielded a considerable proportion of vacancies at the *A* site, as is evident from the refined formula $(Ca_{0.6}La_{0.2}\square_{0.2})$ $(Ce_{0.5}La_{0.12}Nd_{0.15}Dy_{0.10}Pr_{0.05}Sm_{0.02}\square_{0.07})$ $(Mg_{0.40}Fe_{0.15}Cr_{0.12}Ti_{0.12}V_{0.09}Al_{0.12})AlMn$ $(SiO_4)(Si_2O_7)(OH)(F_{0.63}O_{0.37})$ (Sokolova *et al.* 1991). In addition, from their chemical

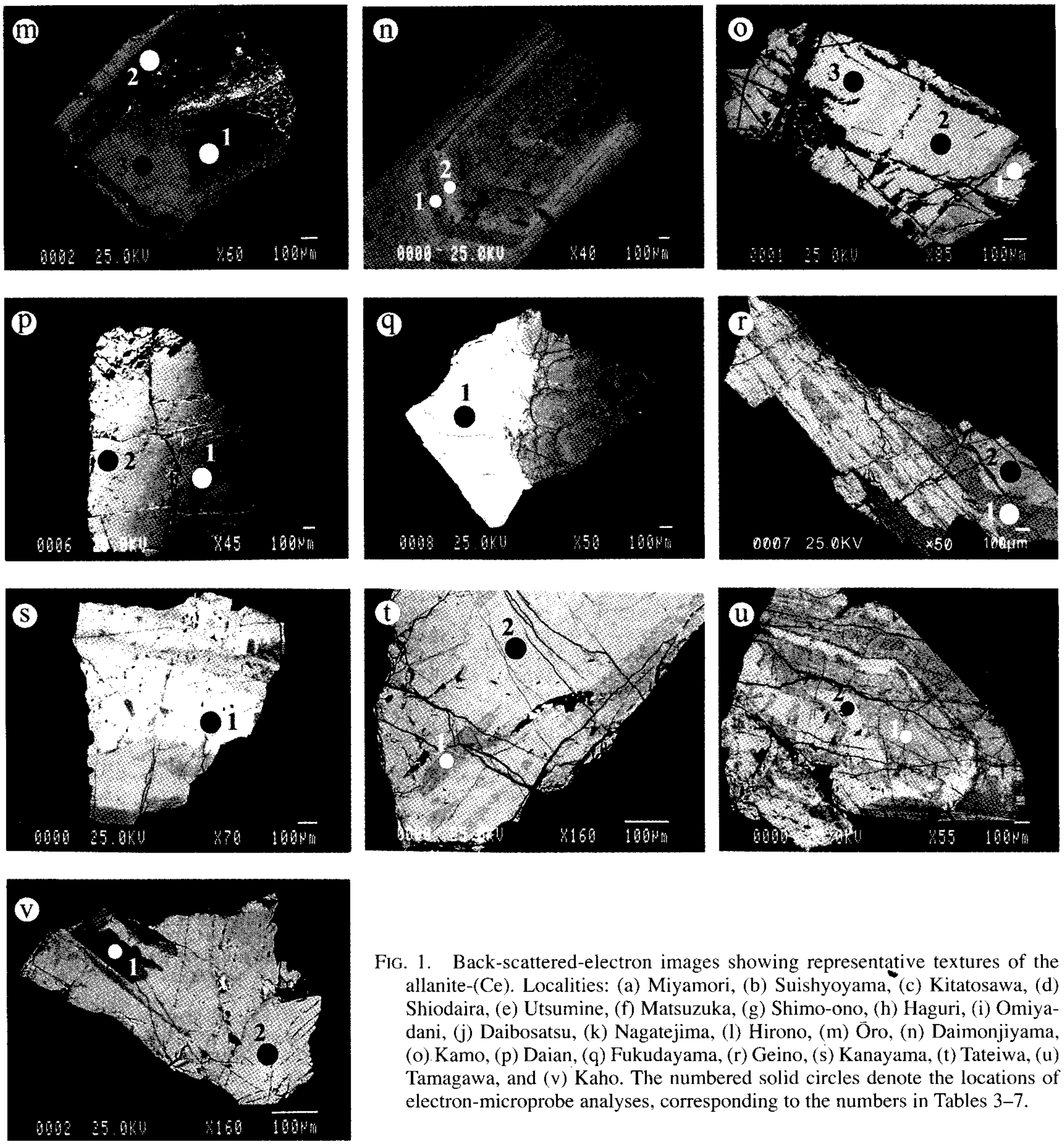

FIG. 1. Back-scattered-electron images showing representative textures of the allanite-(Ce). Localities: (a) Miyamori, (b) Suishyoyama, (c) Kitatosawa, (d) Shiodaira, (e) Utsumine, (f) Matsuzuka, (g) Shimo-ono, (h) Haguri, (i) Omiyadani, (j) Daibosatsu, (k) Nagatejima, (l) Hirono, (m) Ōro, (n) Daimonjiyama, (o) Kamo, (p) Daian, (q) Fukudayama, (r) Geino, (s) Kanayama, (t) Tateiwa, (u) Tamagawa, and (v) Kaho. The numbered solid circles denote the locations of electron-microprobe analyses, corresponding to the numbers in Tables 3–7.

compositions, Peterson & MacFarlane (1993) also estimated varying degrees of vacancy at the *A* site of most of the allanite samples they investigated from granitic rocks and calcite veins in the Grenville Province, Ontario, Canada. Furthermore, these vacancies were interpreted as a result of an omission-type substitution: $3Ca^{2+} = 2REE^{3+} + \square$, where the proportion of the vacancy ranges from 0.059 to 0.439 (Peterson & MacFarlane 1993). Our thirteen samples of allanite incorporate appreciable amounts of Mn at the *A* sites. Therefore, the low *A*-site occupancies for some of the samples suggest the following mechanism of incorporation of the vacancy with the maintenance of charge neutrality: $3(Ca, Mn)^{2+} = 2REE^{3+} + \square$ (Fig. 4).

The behavior of REE and Mn in allanite from Japan

Examination of chemical compositions of allanite from granitic rocks in Japan, as explained in the preceding section, leads to the division into Mn-poor and Mn-rich types (Tables 2–7, Figs. 2, 3). The observation that Mn-rich and Mn-poor compositions do not

TABLE 3. REPRESENTATIVE COMPOSITIONS OF ALLANITE-(Ce) FROM MIYAMORI, SUISHYOYAMA, KITATOSAWA AND SHIODAIRA LOCALITIES

Sample	a) Miyamori			b) Suishyoyama		c) Kitatosawa		d) Shiodaira	
Location	1	2	3	1	2	1	2	1	2
n	5	5	5	5	6	5	5	3	3
SiO_2	33.93(0.50)	33.80(0.30)	33.51(0.15)	31.65(0.28)	31.21(0.51)	32.63(0.27)	32.44(0.29)	33.10(0.11)	31.93(0.02)
TiO_2	1.26(0.03)	1.20(0.03)	1.54(0.02)	<0.003	<0.003	0.88(0.02)	0.92(0.02)	0.04(0.00)	0.10(0.02)
Al_2O_3	15.07(0.19)	14.85(0.09)	14.22(0.08)	15.36(0.13)	15.31(0.04)	17.64(0.06)	17.45(0.04)	21.21(0.01)	20.32(0.03)
Fe_2O_3	11.21(0.11)	11.30(0.10)	11.55(0.06)	9.93(0.19)	9.30(0.11)	11.60(0.09)	11.55(0.16)	8.76(0.13)	9.56(0.02)
FeO	4.10(0.11)	4.34(0.10)	4.34(0.06)	5.40(0.05)	7.16(0.10)	3.76(0.08)	3.84(0.14)	3.65(0.13)	3.51(0.02)
MnO	0.54(0.01)	0.51(0.01)	0.54(0.00)	7.00(0.05)	7.64(0.06)	0.74(0.02)	0.76(0.01)	1.42(0.05)	1.94(0.07)
MgO	1.35(0.02)	1.27(0.12)	1.52(0.02)	<0.002	<0.002	0.37(0.01)	0.36(0.01)	0.10(0.01)	0.15(0.01)
CaO	11.79(0.03)	11.47(0.04)	11.12(0.08)	3.59(0.06)	3.67(0.02)	11.83(0.06)	11.90(0.02)	12.47(0.05)	11.02(0.01)
Sc_2O_3	<0.002	<0.002	<0.002	<0.002	<0.002	<0.002	<0.002	<0.002	<0.002
Y_2O_3	<0.10	<0.10	<0.10	1.61(0.06)	1.56(0.02)	0.67(0.04)	0.70(0.03)	<0.10	<0.10
La_2O_3	5.14(0.08)	5.28(0.12)	5.68(0.06)	2.75(0.10)	3.00(0.00)	4.30(0.09)	4.14(0.08)	2.63(0.03)	3.16(0.04)
Ce_2O_3	7.65(0.05)	7.97(0.07)	8.16(0.13)	7.38(0.24)	7.74(0.27)	7.02(0.15)	6.80(0.06)	6.01(0.01)	6.10(0.44)
Pr_2O_3	1.29(0.07)	1.26(0.04)	1.30(0.01)	1.45(0.06)	1.55(0.04)	1.11(0.05)	1.08(0.05)	1.18(0.01)	1.34(0.06)
Nd_2O_3	3.21(0.03)	3.22(0.00)	3.26(0.03)	4.93(0.06)	5.39(0.00)	3.55(0.02)	3.56(0.07)	3.87(0.01)	4.25(0.06)
Sm_2O_3	0.82(0.02)	0.80(0.02)	0.81(0.01)	1.79(0.03)	1.86(0.04)	0.70(0.01)	0.76(0.08)	2.85(0.07)	3.05(0.01)
Gd_2O_3	<0.22	<0.22	<0.22	1.46(0.06)	1.55(0.00)	0.76(0.01)	0.79(0.04)	2.09(0.04)	1.98(0.04)
Tb_2O_3	<0.15	<0.15	<0.15	<0.15	<0.15	<0.15	<0.15	<0.15	<0.15
Dy_2O_3	<0.22	<0.22	<0.22	<0.22	<0.22	<0.22	<0.22	<0.22	<0.22
Er_2O_3	<0.13	<0.13	<0.13	<0.13	<0.13	<0.13	<0.13	<0.13	<0.13
Tm_2O_3	<0.12	<0.12	<0.12	<0.12	<0.12	<0.12	<0.12	<0.12	<0.12
Yb_2O_3	<0.11	<0.11	<0.11	<0.11	<0.11	<0.11	<0.11	<0.11	<0.11
ThO_2	2.41(0.04)	2.65(0.04)	2.75(0.08)	1.62(0.04)	1.48(0.02)	1.48(0.00)	1.40(0.02)	0.24(0.00)	0.28(0.02)
Na_2O	<0.04	<0.04	<0.04	<0.04	<0.04	<0.04	<0.04	<0.04	<0.04
K_2O	<0.01	<0.01	<0.01	<0.01	<0.01	<0.01	<0.01	<0.01	<0.01
Total	99.77	99.92	100.30	95.92	98.42	99.04	98.45	99.62	98.69
Si	3.060(0.040)	3.061(0.065)	3.046(0.048)	3.076(0.033)	3.009(0.044)	2.944(0.022)	2.943(0.024)	2.924(0.019)	2.889(0.009)
^{T}Al	0.000	0.000	0.000	0.000	0.000	0.056(0.000)	0.057(0.000)	0.076(0.000)	0.111(0.000)
Total *T*	3.060	3.061	3.046	3.076	3.009	3.000	3.000	3.000	3.000
Ti	0.085(0.024)	0.082(0.004)	0.105(0.002)	0.000	0.000	0.060(0.003)	0.063(0.002)	0.002(0.000)	0.007(0.002)
^{M}Al	1.603(0.013)	1.586(0.015)	1.524(0.007)	1.759(0.018)	1.739(0.021)	1.819(0.014)	1.809(0.012)	2.132(0.003)	2.056(0.009)
Fe^{3+}	0.761(0.017)	0.770(0.014)	0.790(0.007)	0.726(0.010)	0.577(0.036)	0.788(0.014)	0.788(0.022)	0.582(0.007)	0.651(0.001)
Fe^{2+}	0.309(0.017)	0.329(0.014)	0.330(0.007)	0.439(0.011)	0.675(0.039)	0.283(0.016)	0.290(0.024)	0.270(0.007)	0.266(0.001)
^{M}Mn	0.000	0.000	0.000	0.000	0.000	0.000	0.000	0.000	0.000
Mg	0.182(0.005)	0.172(0.034)	0.205(0.004)	0.000	0.000	0.050(0.002)	0.050(0.002)	0.014(0.003)	0.020(0.003)
Total *M*	2.940	2.939	2.954	2.924	2.991	3.000	3.000	3.000	3.000
Ca	1.139(0.010)	1.113(0.009)	1.083(0.013)	0.374(0.013)	0.379(0.023)	1.144(0.020)	1.157(0.008)	1.180(0.009)	1.068(0.003)
^{A}Mn	0.041(0.002)	0.039(0.002)	0.042(0.001)	0.576(0.012)	0.624(0.000)	0.057(0.003)	0.058(0.002)	0.106(0.007)	0.149(0.004)
Sc	0.000	0.000	0.000	0.000	0.000	0.000	0.000	0.000	0.000
Y	0.000	0.000	0.000	0.083(0.006)	0.080(0.003)	0.032(0.004)	0.034(0.003)	0.000	0.000
La	0.171(0.009)	0.176(0.008)	0.190(0.003)	0.099(0.008)	0.107(0.002)	0.143(0.006)	0.139(0.007)	0.086(0.002)	0.105(0.003)
Ce	0.253(0.003)	0.264(0.006)	0.272(0.007)	0.263(0.017)	0.273(0.015)	0.232(0.008)	0.226(0.004)	0.194(0.001)	0.202(0.028)
Pr	0.043(0.005)	0.042(0.003)	0.043(0.001)	0.051(0.004)	0.054(0.003)	0.036(0.004)	0.036(0.003)	0.038(0.000)	0.044(0.004)
Nd	0.103(0.001)	0.104(0.000)	0.106(0.001)	0.171(0.003)	0.186(0.003)	0.114(0.002)	0.115(0.004)	0.122(0.000)	0.137(0.004)
Sm	0.026(0.001)	0.025(0.002)	0.025(0.001)	0.060(0.003)	0.062(0.002)	0.022(0.000)	0.024(0.005)	0.087(0.004)	0.095(0.001)
Gd	0.000	0.000	0.000	0.047(0.004)	0.050(0.001)	0.023(0.001)	0.024(0.003)	0.061(0.002)	0.058(0.003)
Tb	0.000	0.000	0.000	0.000	0.000	0.000	0.000	0.000	0.000
Dy	0.000	0.000	0.000	0.000	0.000	0.000	0.000	0.000	0.000
Er	0.000	0.000	0.000	0.000	0.000	0.000	0.000	0.000	0.000
Tm	0.000	0.000	0.000	0.000	0.000	0.000	0.000	0.000	0.000
Yb	0.000	0.000	0.000	0.000	0.000	0.000	0.000	0.000	0.000
Th	0.049(0.001)	0.055(0.002)	0.057(0.003)	0.036(0.002)	0.032(0.000)	0.030(0.000)	0.029(0.001)	0.005(0.003)	0.006(0.003)
Na	0.000	0.000	0.000	0.000	0.000	0.000	0.000	0.000	0.000
K	0.000	0.000	0.000	0.000	0.000	0.000	0.000	0.000	0.000
Total *A*	1.825	1.818	1.818	1.760	1.847	1.833	1.842	1.879	1.864

See Figures 1a-d for spot locations. *n*: number of microprobe points. Number in parentheses is standard deviation. The compositions are first reported in wt%, then the proportion of cations is reported in atoms per formula unit (*apfu*).

TABLE 4. REPRESENTATIVE COMPOSITIONS OF ALLANITE-(Ce) FROM UTSUMINE, MATSUZUKA, SHIMO-ONO, HAGURI AND OMIYADANI

Sample	e) Utsumine		f) Matsuzuka	g) Shimo-ono	h) Haguri		i) Omiyadani		
Location	1	2	1	1	1	2	1	2	3
n	5	5	8	8	5	5	3	5	3
SiO_2	33.32(0.21)	33.01(0.26)	33.23(0.94)	32.43(0.64)	31.44(0.20)	31.23(0.12)	33.77(0.21)	34.18(0.00)	33.53(0.23)
TiO_2	0.70(0.04)	0.84(0.04)	0.29(0.01)	0.80(0.06)	<0.003	<0.003	1.03(0.01)	1.10(0.02)	0.47(0.02)
Al_2O_3	16.07(0.07)	15.39(0.09)	18.21(0.08)	14.50(0.12)	15.96(0.07)	15.83(0.11)	17.66(0.55)	18.27(0.08)	18.02(0.24)
Fe_2O_3	7.80(0.10)	7.50(0.10)	12.44(0.08)	8.64(0.18)	10.99(0.16)	12.60(0.28)	12.61(0.88)	8.63(0.67)	11.76(0.12)
FeO	5.95(0.11)	7.01(0.09)	2.20(0.07)	8.47(0.16)	5.35(0.14)	4.35(0.38)	1.16(0.79)	3.62(0.60)	2.45(0.12)
MnO	2.80(0.01)	2.79(0.02)	2.28(0.05)	4.52(0.01)	6.61(0.03)	7.31(0.12)	0.25(0.00)	0.54(0.01)	0.89(0.01)
MgO	0.57(0.11)	0.65(0.04)	<0.002	0.15(0.00)	<0.002	<0.002	1.05(0.21)	0.73(0.11)	0.50(0.04)
CaO	10.67(0.03)	10.61(0.08)	9.25(0.08)	7.76(0.03)	3.13(0.04)	2.33(0.02)	10.29(0.46)	11.38(0.06)	9.52(0.13)
Sc_2O_3	0.44(0.01)	0.50(0.06)	0.12(0.01)	<0.002	<0.002	<0.002	<0.002	<0.002	<0.002
Y_2O_3	0.54(0.04)	0.43(0.04)	<0.10	1.13(0.01)	1.93(0.05)	1.90(0.09)	<0.10	<0.10	<0.10
La_2O_3	3.03(0.03)	3.30(0.07)	2.72(0.11)	2.39(0.01)	2.28(0.07)	2.26(0.14)	6.66(0.37)	5.54(0.05)	6.08(0.11)
Ce_2O_3	6.77(0.09)	6.86(0.34)	6.07(0.45)	5.68(0.00)	6.65(0.05)	6.66(0.12)	9.35(0.34)	8.12(0.09)	9.03(0.07)
Pr_2O_3	1.40(0.02)	1.38(0.12)	1.28(0.02)	1.27(0.00)	1.48(0.05)	1.52(0.06)	1.28(0.05)	1.20(0.03)	1.42(0.03)
Nd_2O_3	4.22(0.06)	4.22(0.03)	4.89(0.05)	5.30(0.01)	6.20(0.12)	6.26(0.16)	3.37(0.03)	3.42(0.01)	4.13(0.09)
Sm_2O_3	1.67(0.03)	1.55(0.04)	1.36(0.01)	1.93(0.00)	2.87(0.09)	2.88(0.14)	0.56(0.01)	0.64(0.01)	0.80(0.04)
Gd_2O_3	1.15(0.03)	1.02(0.05)	1.08(0.01)	1.46(0.00)	2.08(0.06)	2.21(0.05)	<0.22	<0.22	<0.22
Tb_2O_3	<0.15	<0.15	<0.15	<0.15	<0.15	<0.15	<0.15	<0.15	<0.15
Dy_2O_3	<0.22	<0.22	0.40(0.01)	0.54(0.00)	0.86(0.03)	0.84(0.06)	<0.22	<0.22	<0.22
Er_2O_3	<0.13	<0.13	0.21(0.01)	<0.13	<0.13	<0.13	<0.13	<0.13	<0.13
Tm_2O_3	<0.12	<0.12	<0.12	<0.12	<0.12	<0.12	<0.12	<0.12	<0.12
Yb_2O_3	<0.11	<0.11	0.18(0.02)	<0.11	<0.11	<0.11	<0.11	<0.11	<0.11
ThO_2	1.55(0.02)	1.83(0.05)	2.19(0.01)	3.11(0.07)	1.76(0.05)	1.48(0.08)	0.97(0.02)	1.59(0.02)	1.61(0.10)
Na_2O	<0.04	<0.04	<0.04	<0.04	<0.04	<0.04	<0.04	<0.04	<0.04
K_2O	<0.01	<0.01	<0.01	<0.01	<0.01	<0.01	<0.01	<0.01	<0.01
Total	98.65	98.89	98.40	100.08	99.59	99.66	100.01	98.96	100.21
Si	3.060(0.060)	3.050(0.060)	3.015(0.093)	3.044(0.057)	2.994(0.018)	2.974(0.040)	3.007(0.010)	3.054(0.040)	3.013(0.006)
^{T}Al	0.000	0.000	0.000	0.000	0.006(0.000)	0.026(0.000)	0.000	0.000	0.000
Total *T*	3.060	3.050	3.015	3.044	3.000	3.000	3.007	3.054	3.013
Ti	0.049(0.005)	0.058(0.006)	0.020(0.092)	0.056(0.009)	0.000	0.000	0.069(0.002)	0.074(0.004)	0.032(0.003)
^{M}Al	1.739(0.008)	1.676(0.016)	1.948(0.062)	1.604(0.016)	1.786(0.016)	1.751(0.007)	1.853(0.088)	1.924(0.003)	1.908(0.026)
Fe^{3+}	0.539(0.012)	0.522(0.059)	0.850(0.028)	0.610(0.029)	0.788(0.012)	0.903(0.077)	0.845(0.127)	0.580(0.077)	0.795(0.019)
Fe^{2+}	0.457(0.012)	0.542(0.060)	0.167(0.030)	0.665(0.032)	0.426(0.014)	0.346(0.050)	0.086(0.137)	0.271(0.083)	0.184(0.021)
^{M}Mn	0.078(0.000)	0.062(0.000)	0.000	0.000	0.000	0.000	0.000	0.000	0.000
Mg	0.078(0.031)	0.090(0.010)	0.000	0.021(0.004)	0.000	0.000	0.139(0.054)	0.097(0.029)	0.067(0.012)
Total *M*	2.940	2.950	2.985	2.956	3.000	3.000	2.993	2.946	2.987
Ca	1.050(0.009)	1.050(0.014)	0.899(0.019)	0.780(0.032)	0.319(0.009)	0.238(0.000)	0.982(0.074)	1.090(0.000)	0.917(0.014)
^{A}Mn	0.140(0.003)	0.157(0.004)	0.175(0.002)	0.359(0.013)	0.533(0.008)	0.590(0.015)	0.019(0.000)	0.041(0.001)	0.068(0.002)
Sc	0.035(0.001)	0.040(0.009)	0.009(0.000)	0.000	0.000	0.000	0.000	0.000	0.000
Y	0.026(0.004)	0.021(0.004)	0.000	0.056(0.009)	0.098(0.006)	0.096(0.009)	0.000	0.000	0.000
La	0.102(0.002)	0.112(0.006)	0.091(0.009)	0.083(0.006)	0.080(0.005)	0.079(0.009)	0.219(0.029)	0.183(0.006)	0.202(0.005)
Ce	0.227(0.006)	0.232(0.022)	0.202(0.031)	0.195(0.004)	0.232(0.004)	0.232(0.006)	0.305(0.028)	0.266(0.009)	0.297(0.008)
Pr	0.047(0.001)	0.046(0.008)	0.042(0.003)	0.043(0.003)	0.051(0.004)	0.053(0.005)	0.042(0.004)	0.039(0.002)	0.046(0.002)
Nd	0.138(0.004)	0.139(0.003)	0.158(0.001)	0.178(0.005)	0.211(0.008)	0.213(0.011)	0.107(0.004)	0.109(0.002)	0.133(0.008)
Sm	0.053(0.002)	0.049(0.003)	0.043(0.002)	0.062(0.003)	0.094(0.005)	0.095(0.011)	0.017(0.001)	0.020(0.001)	0.025(0.002)
Gd	0.035(0.002)	0.031(0.003)	0.032(0.001)	0.045(0.003)	0.066(0.004)	0.070(0.004)	0.000	0.000	0.000
Tb	0.000	0.000	0.000	0.000	0.000	0.000	0.000	0.000	0.000
Dy	0.000	0.000	0.012(0.001)	0.016(0.004)	0.026(0.002)	0.026(0.004)	0.000	0.000	0.000
Er	0.000	0.000	0.006(0.001)	0.000	0.000	0.000	0.000	0.000	0.000
Tm	0.000	0.000	0.000	0.000	0.000	0.000	0.000	0.000	0.000
Yb	0.000	0.000	0.005(0.002)	0.000	0.000	0.000	0.000	0.000	0.000
Th	0.032(0.001)	0.038(0.002)	0.045(0.019)	0.066(0.007)	0.038(0.002)	0.032(0.004)	0.020(0.001)	0.032(0.001)	0.033(0.005)
Na	0.000	0.000	0.000	0.000	0.000	0.000	0.000	0.000	0.000
K	0.000	0.000	0.000	0.000	0.000	0.000	0.000	0.000	0.000
Total *A*	1.885	1.915	1.719	1.883	1.748	1.724	1.711	1.780	1.721

See Figures 1e-i for spot locations. *n*: number of microprobe points. Number in parentheses is standard deviation. The compositions are first reported in wt%, then the proportion of cations is reported in atoms per formula unit (*apfu*).

TABLE 5. REPRESENTATIVE COMPOSITIONS OF ALLANITE-(Ce) FROM DAIBOSATSU, NAGATEJIMA, HIRONO AND ORO

Sample	j) Daibosatsu	k) Nagatejima			l) Hirono		m) Ōro		
Location	1	1	2	3	1*	2	1	2	3
n	8	3	3	3	3	8	5	5	5
SiO_2	31.05(0.15)	35.58(0.74)	33.12(1.54)	35.22(0.94)	37.98(0.25)	33.74(0.48)	32.96(0.34)	31.58(0.97)	31.21(0.23)
TiO_2	1.11(0.05)	0.56(0.03)	0.68(0.05)	0.58(0.01)	0.29(0.03)	0.82(0.12)	1.92(0.01)	1.64(0.05)	1.54(0.01)
Al_2O_3	14.53(0.20)	18.41(0.00)	17.77(0.29)	16.13(0.21)	23.03(0.30)	17.07(0.48)	13.32(0.13)	12.89(0.13)	13.01(0.39)
Fe_2O_3	6.65(0.03)	14.52(0.03)	13.12(0.24)	15.52(0.08)	8.65(0.25)	8.05(0.36)	15.91(0.11)	7.79(0.08)	7.04(0.10)
FeO	8.83(0.03)	0.40(0.03)	1.60(0.22)	0.00(0.07)	3.49(0.25)	5.96(0.35)	0.00(0.10)	8.60(0.07)	10.50(0.09)
MnO	0.88(0.03)	0.55(0.00)	0.71(0.03)	1.74(0.01)	0.26(0.01)	0.71(0.03)	3.60(0.12)	3.62(0.01)	3.52(0.03)
MgO	0.52(0.05)	0.94(0.01)	1.11(0.14)	1.28(0.05)	<0.002	<0.002	0.70(0.02)	0.68(0.04)	0.76(0.05)
CaO	8.55(0.03)	13.08(0.15)	11.90(0.13)	9.34(0.11)	20.93(0.25)	12.29(0.30)	7.49(0.06)	7.57(0.04)	9.19(0.04)
Sc_2O_3	<0.002	<0.002	<0.002	<0.002	<0.002	<0.002	<0.002	<0.002	<0.002
Y_2O_3	<0.10	<0.10	<0.10	<0.10	2.30(0.27)	<0.10	1.00(0.01)	0.80(0.05)	0.77(0.04)
La_2O_3	6.79(0.08)	3.98(0.02)	4.51(0.13)	5.26(0.05)	<0.11	3.26(0.05)	3.23(0.02)	4.12(0.04)	3.90(0.10)
Ce_2O_3	12.98(0.06)	6.60(0.05)	7.41(0.07)	8.62(0.12)	0.22(0.04)	8.20(0.37)	7.13(0.04)	8.34(0.10)	8.33(0.08)
Pr_2O_3	1.42(0.01)	1.09(0.07)	1.20(0.04)	1.27(0.05)	<0.13	1.67(0.06)	1.25(0.09)	1.40(0.04)	1.44(0.03)
Nd_2O_3	3.13(0.00)	3.15(0.02)	3.21(0.05)	3.87(0.07)	0.51(0.07)	5.19(0.07)	4.22(0.05)	4.32(0.03)	4.56(0.07)
Sm_2O_3	0.77(0.05)	0.67(0.02)	0.70(0.06)	0.73(0.01)	0.71(0.03)	1.06(0.03)	1.24(0.01)	1.12(0.01)	1.37(0.04)
Gd_2O_3	<0.22	0.41(0.03)	0.48(0.06)	0.57(0.04)	1.03(0.01)	0.71(0.01)	1.17(0.05)	1.04(0.10)	1.19(0.03)
Tb_2O_3	<0.15	<0.15	<0.15	<0.15	<0.15	<0.15	<0.15	<0.15	<0.15
Dy_2O_3	<0.22	0.32(0.04)	0.40(0.05)	0.42(0.01)	0.50(0.06)	0.26(0.02)	<0.22	<0.22	<0.22
Er_2O_3	<0.13	<0.13	<0.13	<0.13	<0.13	<0.13	<0.13	<0.13	<0.13
Tm_2O_3	<0.12	<0.12	<0.12	<0.12	<0.12	<0.12	<0.12	<0.12	<0.11
Yb_2O_3	<0.11	<0.11	<0.11	<0.11	<0.11	<0.11	<0.11	<0.11	<0.11
ThO_2	1.66(0.03)	1.37(0.05)	2.08(0.10)	1.30(0.10)	<0.01	<0.01	2.63(0.04)	2.30(0.08)	1.70(0.05)
Na_2O	<0.04	<0.04	<0.04	<0.04	<0.04	<0.04	<0.04	<0.04	<0.04
K_2O	<0.01	<0.01	<0.01	<0.01	<0.01	<0.01	<0.01	<0.01	<0.01
Total	98.87	101.63	100.00	101.85	99.90	98.99	97.77	97.81	100.03
Si	2.997(0.007)	3.034(0.066)	2.946(0.169)	3.087(0.100)	3.046(0.042)	3.062(0.060)	3.068(0.030)	3.053(0.111)	2.976(0.015)
^{T}Al	0.003(0.000)	0.000	0.054(0.000)	0.000	0.000	0.000	0.000	0.000	0.024(0.000)
Total *T*	3.000	3.034	3.000	3.087	3.046	3.062	3.068	3.053	3.031
Ti	0.080(0.079)	0.036(0.003)	0.046(0.007)	0.038(0.001)	0.018(0.004)	0.056(0.017)	0.134(0.004)	0.119(0.005)	0.110(0.003)
^{M}Al	1.649(0.031)	1.850(0.035)	1.810(0.116)	1.666(0.020)	2.180(0.061)	1.825(0.087)	1.462(0.027)	1.469(0.063)	1.439(0.064)
Fe^{3+}	0.483(0.015)	0.932(0.016)	0.878(0.023)	1.024(0.006)	0.522(0.030)	0.550(0.066)	1.114(0.014)	0.567(0.044)	0.505(0.028)
Fe^{2+}	0.713(0.015)	0.029(0.017)	0.119(0.025)	0.000(0.007)	0.234(0.030)	0.452(0.066)	0.000(0.016)	0.695(0.049)	0.837(0.031)
^{M}Mn	0.000	0.000	0.000	0.017(0.000)	0.000	0.055(0.006)	0.125(0.000)	0.000	0.000
Mg	0.075(0.014)	0.119(0.001)	0.147(0.038)	0.167(0.010)	0.000	0.000	0.097(0.007)	0.098(0.024)	0.109(0.015)
Total *M*	3.000	2.966	3.000	2.913	2.954	2.938	2.932	2.948	3.000
Ca	0.884(0.012)	1.195(0.049)	1.134(0.064)	0.877(0.033)	1.799(0.038)	1.195(0.052)	0.747(0.009)	0.784(0.029)	0.939(0.014)
^{A}Mn	0.072(0.007)	0.040(0.000)	0.054(0.005)	0.112(0.000)	0.017(0.018)	0.000	0.158(0.018)	0.296(0.008)	0.284(0.007)
Sc	0.000	0.000	0.000	0.000	0.000	0.000	0.000	0.000	0.000
Y	0.000	0.000	0.000	0.000	0.098(0.024)	0.000	0.050(0.001)	0.041(0.005)	0.039(0.004)
La	0.242(0.005)	0.125(0.004)	0.148(0.003)	0.170(0.001)	0.000	0.109(0.002)	0.111(0.003)	0.147(0.002)	0.137(0.009)
Ce	0.459(0.003)	0.206(0.001)	0.241(0.007)	0.277(0.003)	0.006(0.002)	0.272(0.028)	0.243(0.002)	0.295(0.013)	0.291(0.009)
Pr	0.050(0.008)	0.034(0.005)	0.039(0.004)	0.041(0.002)	0.000	0.055(0.005)	0.042(0.006)	0.049(0.003)	0.050(0.002)
Nd	0.108(0.000)	0.096(0.000)	0.102(0.001)	0.121(0.003)	0.015(0.004)	0.168(0.006)	0.140(0.003)	0.149(0.006)	0.155(0.002)
Sm	0.026(0.001)	0.020(0.001)	0.021(0.004)	0.022(0.001)	0.019(0.002)	0.033(0.002)	0.040(0.001)	0.037(0.002)	0.045(0.003)
Gd	0.000	0.012(0.001)	0.014(0.004)	0.017(0.002)	0.031(0.000)	0.021(0.001)	0.036(0.003)	0.033(0.007)	0.038(0.001)
Tb	0.000	0.000	0.000	0.000	0.000	0.000	0.000	0.000	0.000
Dy	0.000	0.009(0.002)	0.011(0.003)	0.012(0.000)	0.015(0.004)	0.008(0.002)	0.000	0.000	0.000
Er	0.000	0.000	0.000	0.000	0.000	0.000	0.000	0.000	0.000
Tm	0.000	0.000	0.000	0.000	0.000	0.000	0.000	0.000	0.000
Yb	0.000	0.000	0.000	0.000	0.000	0.000	0.000	0.000	0.000
Th	0.036(0.002)	0.027(0.002)	0.042(0.004)	0.026(0.004)	0.000	0.000	0.056(0.001)	0.051(0.002)	0.037(0.002)
Na	0.000	0.000	0.000	0.000	0.000	0.000	0.000	0.000	0.000
K	0.000	0.000	0.000	0.000	0.000	0.000	0.000	0.000	0.000
Total *A*	1.877	1.764	1.806	1.675	2.000	1.861	1.623	1.882	2.015

See Figures 1j–m for spot locations. * According to the definition used by Pan & Fleet (1991), allanite requires at least 50% occupancy of the *A*2 site by total rare-earth elements (REE), corresponding to 15 wt%. Therefore, the data on the sample from Hirono in column 1* pertain to REE-rich epidote. *n*: number of microprobe points. Number in parentheses is standard deviation. The compositions are first reported in wt%, then the proportion of cations is reported in atoms per formula unit (*apfu*).

TABLE 6. REPRESENTATIVE COMPOSITIONS OF ALLANITE-(Ce) FROM DAIMONJIYAMA, KAMO, DAIAN AND FUKUDAYAMA

Sample	n) Daimonjiyama		o) Kamo			p) Daian		q) Fukudayama
Location	1	2	1	2	3	1	2	1
n	5	4	5	5	5	5	5	8
SiO_2	34.33(0.19)	34.36(0.27)	34.37(0.18)	34.46(0.15)	34.60(0.10)	32.06(0.16)	31.90(0.29)	34.09(1.03)
TiO_2	1.08(0.04)	0.53(0.03)	0.13(0.01)	0.13(0.00)	0.13(0.00)	1.59(0.01)	1.50(0.15)	0.05(0.01)
Al_2O_3	17.37(0.41)	18.19(0.17)	18.13(0.04)	18.12(0.11)	18.12(0.09)	16.90(0.04)	15.47(0.27)	17.97(0.38)
Fe_2O_3	11.86(0.07)	11.40(0.15)	11.10(0.01)	11.24(0.06)	11.80(0.22)	11.43(0.09)	6.08(0.48)	10.78(0.26)
FeO	1.65(0.06)	1.82(0.14)	3.60(0.26)	3.65(0.05)	3.15(0.19)	2.67(0.08)	8.27(0.43)	3.98(0.24)
MnO	0.23(0.02)	0.78(0.07)	2.11(0.01)	2.17(0.02)	2.12(0.00)	1.01(0.05)	1.05(0.03)	2.05(0.09)
MgO	0.99(0.02)	0.67(0.01)	0.16(0.02)	0.17(0.01)	0.18(0.00)	0.46(0.01)	0.56(0.02)	<0.002
CaO	10.23(0.08)	9.74(0.16)	8.99(0.04)	8.95(0.01)	8.90(0.05)	7.96(0.02)	9.40(0.10)	8.52(0.14)
Sc_2O_3	<0.002	<0.002	<0.002	<0.002	<0.002	<0.002	<0.002	0.11(0.01)
Y_2O_3	<0.10	<0.10	0.98(0.02)	1.04(0.08)	1.03(0.07)	0.71(0.02)	0.92(0.04)	2.19(0.24)
La_2O_3	6.81(0.15)	5.75(0.24)	3.34(0.07)	3.33(0.05)	3.26(0.06)	4.48(0.05)	5.07(0.06)	2.67(0.17)
Ce_2O_3	9.40(0.08)	8.91(0.07)	6.50(0.24)	6.65(0.09)	6.59(0.03)	7.90(0.19)	8.16(0.05)	5.39(0.20)
Pr_2O_3	1.20(0.05)	1.34(0.04)	1.23(0.05)	1.25(0.04)	1.21(0.05)	1.33(0.04)	1.38(0.03)	0.99(0.05)
Nd_2O_3	3.34(0.06)	3.96(0.05)	4.77(0.06)	4.66(0.03)	4.69(0.06)	4.02(0.04)	4.35(0.10)	3.93(0.06)
Sm_2O_3	0.42(0.02)	0.66(0.04)	1.49(0.06)	1.46(0.01)	1.47(0.04)	0.99(0.01)	0.17(0.02)	1.85(0.06)
Gd_2O_3	0.25(0.014)	0.43(0.07)	1.32(0.03)	1.33(0.03)	1.37(0.03)	1.02(0.05)	1.07(0.09)	1.94(0.09)
Tb_2O_3	<0.15	<0.15	<0.15	<0.15	<0.15	<0.15	<0.15	<0.15
Dy_2O_3	<0.22	<0.22	0.50(0.03)	0.49(0.01)	0.46(0.01)	0.53(0.03)	0.62(0.04)	0.85(0.07)
Er_2O_3	<0.13	<0.13	<0.13	<0.13	<0.13	<0.13	<0.13	<0.13
Tm_2O_3	<0.12	<0.12	<0.12	<0.12	<0.12	<0.12	<0.12	<0.12
Yb_2O_3	<0.11	<0.11	<0.11	<0.11	<0.11	<0.11	<0.11	<0.11
ThO_2	0.68(0.03)	1.21(0.14)	2.65(0.07)	2.78(0.04)	2.76(0.07)	3.64(0.05)	3.23(0.08)	2.95(0.24)
Na_2O	<0.04	<0.04	<0.04	<0.04	<0.04	<0.04	<0.04	<0.04
K_2O	<0.01	<0.01	<0.01	<0.01	<0.01	<0.01	<0.01	<0.01
Total	99.84	99.75	101.37	101.88	101.84	98.70	99.20	100.31
Si	3.056(0.050)	3.063(0.040)	3.058(0.030)	3.055(0.021)	3.060(0.015)	2.973(0.005)	3.010(0.035)	3.065(0.118)
^{T}Al	0.000	0.000	0.000	0.000	0.000	0.027(0.000)	0.000	0.000
Total *T*	3.056	3.063	3.058	3.055	3.060	3.000	3.010	3.065
Ti	0.072(0.005)	0.036(0.004)	0.009(0.001)	0.009(0.000)	0.009(0.000)	0.111(0.002)	0.106(0.020)	0.003(0.001)
^{M}Al	1.822(0.066)	1.911(0.033)	1.901(0.014)	1.893(0.012)	1.889(0.021)	1.820(0.007)	1.720(0.022)	1.904(0.120)
Fe^{3+}	0.794(0.012)	0.765(0.016)	0.743(0.005)	0.750(0.014)	0.785(0.026)	0.798(0.006)	0.432(0.045)	0.729(0.036)
Fe^{2+}	0.123(0.013)	0.136(0.017)	0.268(0.005)	0.271(0.016)	0.233(0.028)	0.207(0.006)	0.653(0.049)	0.299(0.039)
^{M}Mn	0.000	0.000	0.000	0.000	0.000	0.000	0.000	0.000
Mg	0.131(0.005)	0.089(0.001)	0.021(0.005)	0.022(0.002)	0.024(0.004)	0.064(0.003)	0.079(0.005)	0.000
Total *M*	2.942	2.937	2.942	2.945	2.940	3.000	2.990	2.935
Ca	0.976(0.010)	0.940(0.038)	0.857(0.005)	0.850(0.007)	0.843(0.008)	0.791(0.004)	0.950(0.011)	0.821(0.042)
^{A}Mn	0.017(0.003)	0.060(0.009)	0.159(0.002)	0.163(0.002)	0.159(0.002)	0.079(0.000)	0.084(0.004)	0.156(0.012)
Sc	0.000	0.000	0.000	0.000	0.000	0.000	0.000	0.009(0.002)
Y	0.000	0.000	0.046(0.001)	0.049(0.007)	0.048(0.007)	0.035(0.002)	0.046(0.005)	0.105(0.024)
La	0.224(0.012)	0.191(0.016)	0.110(0.004)	0.109(0.004)	0.106(0.004)	0.153(0.004)	0.176(0.002)	0.089(0.011)
Ce	0.306(0.007)	0.294(0.005)	0.212(0.016)	0.216(0.004)	0.213(0.002)	0.268(0.011)	0.282(0.009)	0.177(0.013)
Pr	0.039(0.004)	0.044(0.002)	0.040(0.003)	0.040(0.003)	0.039(0.003)	0.045(0.003)	0.047(0.003)	0.032(0.003)
Nd	0.106(0.004)	0.127(0.003)	0.152(0.004)	0.148(0.003)	0.148(0.003)	0.133(0.004)	0.147(0.010)	0.126(0.003)
Sm	0.013(0.002)	0.021(0.002)	0.046(0.004)	0.045(0.001)	0.045(0.003)	0.032(0.001)	0.006(0.002)	0.057(0.004)
Gd	0.007(0.001)	0.013(0.004)	0.039(0.002)	0.039(0.002)	0.040(0.002)	0.031(0.003)	0.033(0.006)	0.058(0.006)
Tb	0.000	0.000	0.000	0.000	0.000	0.000	0.000	0.000
Dy	0.000	0.000	0.014(0.002)	0.014(0.001)	0.013(0.001)	0.016(0.002)	0.019(0.003)	0.025(0.005)
Er	0.000	0.000	0.000	0.000	0.000	0.000	0.000	0.000
Tm	0.000	0.000	0.000	0.000	0.000	0.000	0.000	0.000
Yb	0.000	0.000	0.000	0.000	0.000	0.000	0.000	0.000
Th	0.014(0.001)	0.025(0.005)	0.054(0.003)	0.056(0.002)	0.056(0.003)	0.077(0.003)	0.069(0.005)	0.060(0.010)
Na	0.000	0.000	0.000	0.000	0.000	0.000	0.000	0.000
K	0.000	0.000	0.000	0.000	0.000	0.000	0.000	0.000
Total *A*	1.702	1.715	1.729	1.729	1.710	1.660	1.859	1.715

See Figures 1n–q for spot locations. *n*: number of microprobe points. Number in parentheses is standard deviation. The compositions are first reported in wt%, then the proportion of cations is reported in atoms per formula unit (*apfu*).

TABLE 7. REPRESENTATIVE COMPOSITIONS OF ALLANITE-(Ce) FROM GEINO, KANAYAMA, TATEIWA, TAMAGAWA AND KAHO

Sample	r) Geino		s) Kanayama	t) Tateiwa		u) Tamagawa		v) Kaho	
Location	1	2	1	1	2	1	2	1*	2
n	5	5	5	5	10	5	5	3	8
SiO_2	31.99(0.19)	32.97(0.32)	32.37(1.04)	32.08(0.15)	32.44(0.20)	32.77(0.30)	32.38(0.00)	35.99(0.16)	32.44(0.51)
TiO_2	<0.003	<0.003	<0.003	<0.003	<0.003	0.27(0.01)	0.26(0.00)	0.23(0.02)	1.32(0.03)
Al_2O_3	18.27(0.07)	17.12(0.11)	17.27(0.40)	16.73(0.26)	16.42(0.31)	16.99(0.67)	17.22(0.04)	20.19(0.39)	13.70(0.25)
Fe_2O_3	12.19(0.23)	16.37(0.13)	10.98(0.08)	6.03(0.58)	8.05(0.16)	7.09(0.28)	9.15(0.01)	8.91(0.14)	10.03(0.02)
FeO	1.60(0.26)	0.19(0.13)	4.95(0.07)	8.10(0.53)	6.65(0.15)	6.40(0.25)	5.85(0.00)	4.10(0.13)	6.65(0.02)
MnO	3.82(0.08)	4.67(0.12)	5.24(0.36)	3.87(0.04)	4.41(0.11)	3.26(0.11)	3.30(0.00)	0.57(0.06)	1.44(0.03)
MgO	<0.002	<0.002	<0.002	<0.002	<0.002	<0.002	<0.002	0.11(0.01)	0.70(0.04)
CaO	4.06(0.02)	3.55(0.10)	4.20(0.34)	6.16(0.26)	6.65(0.28)	6.55(0.21)	6.57(0.03)	17.15(0.35)	9.66(0.02)
Sc_2O_3	0.10(0.01)	0.08(0.11)	<0.002	<0.002	<0.002	<0.002	<0.002	<0.002	<0.002
Y_2O_3	1.99(0.04)	1.77(0.00)	3.57(0.52)	3.56(0.10)	3.30(0.12)	2.94(0.10)	2.58(0.00)	0.23(0.00)	0.23(0.01)
La_2O_3	2.31(0.07)	2.32(0.05)	2.10(0.41)	2.68(0.09)	2.63(0.16)	2.06(0.12)	2.62(0.00)	2.53(0.17)	5.82(0.13)
Ce_2O_3	6.08(0.15)	6.29(0.06)	5.39(0.71)	6.24(0.14)	6.27(0.27)	4.97(0.09)	5.96(0.20)	4.56(0.31)	9.39(0.05)
Pr_2O_3	1.31(0.12)	1.37(0.08)	1.17(0.09)	1.16(0.04)	1.11(0.04)	1.18(0.01)	1.32(0.02)	0.60(0.09)	1.24(0.05)
Nd_2O_3	5.98(0.05)	6.22(0.10)	4.85(0.20)	4.45(0.14)	4.49(0.24)	4.60(0.03)	5.01(0.00)	1.71(0.12)	3.20(0.02)
Sm_2O_3	2.73(0.09)	3.09(0.13)	2.18(0.14)	1.93(0.10)	1.55(0.07)	2.44(0.05)	2.50(0.02)	0.29(0.02)	0.64(0.03)
Gd_2O_3	2.08(0.02)	2.20(0.05)	3.00(0.27)	2.03(0.02)	2.06(0.08)	2.89(0.04)	2.82(0.10)	0.40(0.01)	0.68(0.06)
Tb_2O_3	<0.15	<0.15	0.27(0.04)	<0.15	<0.15	<0.15	<0.15	<0.15	<0.15
Dy_2O_3	0.78(0.02)	0.76(0.02)	1.25(0.13)	1.05(0.06)	0.99(0.03)	1.38(0.06)	1.28(0.02)	<0.22	<0.22
Er_2O_3	<0.13	<0.13	0.28(0.04)	<0.13	<0.13	<0.13	<0.13	<0.13	<0.13
Tm_2O_3	<0.12	<0.12	0.28(0.02)	0.24(0.02)	0.26(0.02)	<0.12	<0.12	<0.12	<0.12
Yb_2O_3	<0.11	<0.11	<0.11	<0.11	<0.11	<0.11	<0.11	<0.11	<0.11
ThO_2	2.78(0.03)	1.60(0.05)	1.92(0.20)	1.93(0.02)	1.48(0.07)	1.91(0.07)	1.15(0.01)	0.35(0.04)	1.27(0.07)
Na_2O	<0.04	<0.04	0.23(0.02)	<0.04	<0.04	<0.04	<0.04	<0.04	<0.04
K_2O	0.15(0.01)	<0.01	0.01(0.00)	<0.01	<0.01	<0.01	<0.01	<0.01	<0.01
Total	98.22	100.57	101.51	98.24	99.81	97.70	99.97	97.92	98.41
Si	2.998(0.016)	3.014(0.047)	2.982(0.095)	3.050(0.050)	3.028(0.029)	3.087(0.088)	3.005(0.006)	3.074(0.050)	3.054(0.055)
^{T}Al	0.002(0.000)	0.000	0.018(0.000)	0.000	0.000	0.000	0.000	0.000	0.000
Total T	3.000	3.014	3.000	3.050	3.028	3.087	3.005	3.074	3.054
Ti	0.000	0.000	0.000	0.000	0.000	0.019(0.001)	0.018(0.000)	0.015(0.003)	0.093(0.005)
^{M}Al	2.016(0.015)	1.845(0.030)	1.858(0.079)	1.875(0.039)	1.806(0.060)	1.887(0.125)	1.884(0.005)	2.032(0.074)	1.520(0.043)
Fe^{3+}	0.859(0.030)	1.126(0.021)	0.761(0.035)	0.431(0.065)	0.565(0.025)	0.503(0.036)	0.639(0.003)	0.573(0.019)	0.711(0.026)
Fe^{2+}	0.125(0.020)	0.015(0.021)	0.381(0.035)	0.644(0.071)	0.601(0.027)	0.504(0.033)	0.454(0.003)	0.293(0.021)	0.524(0.028)
^{M}Mn	0.000	0.000	0.000	0.000	0.000	0.000	0.000	0.000	0.000
Mg	0.000	0.000	0.000	0.000	0.000	0.000	0.000	0.014(0.002)	0.098(0.010)
Total M	3.000	2.986	3.000	2.950	2.972	2.913	2.995	2.927	2.946
Ca	0.408(0.005)	0.348(0.019)	0.415(0.076)	0.628(0.042)	0.665(0.053)	0.661(0.045)	0.653(0.004)	1.569(0.061)	0.974(0.018)
^{A}Mn	0.303(0.014)	0.362(0.020)	0.409(0.046)	0.312(0.005)	0.349(0.015)	0.260(0.015)	0.259(0.000)	0.041(0.009)	0.115(0.003)
Sc	0.008(0.001)	0.006(0.011)	0.000	0.000	0.000	0.000	0.000	0.000	0.000
Y	0.099(0.004)	0.086(0.000)	0.175(0.046)	0.180(0.013)	0.164(0.012)	0.147(0.010)	0.127(0.000)	0.010(0.000)	0.012(0.002)
La	0.080(0.005)	0.078(0.004)	0.071(0.029)	0.094(0.008)	0.091(0.011)	0.072(0.010)	0.090(0.000)	0.080(0.011)	0.202(0.006)
Ce	0.209(0.011)	0.211(0.005)	0.182(0.052)	0.217(0.009)	0.214(0.017)	0.171(0.008)	0.203(0.013)	0.143(0.020)	0.324(0.009)
Pr	0.045(0.009)	0.046(0.006)	0.039(0.007)	0.040(0.003)	0.038(0.003)	0.041(0.000)	0.045(0.002)	0.019(0.006)	0.043(0.004)
Nd	0.200(0.004)	0.203(0.007)	0.160(0.018)	0.151(0.009)	0.150(0.015)	0.155(0.001)	0.166(0.001)	0.052(0.008)	0.108(0.004)
Sm	0.088(0.006)	0.097(0.009)	0.069(0.008)	0.063(0.006)	0.050(0.004)	0.079(0.004)	0.080(0.002)	0.009(0.001)	0.021(0.002)
Gd	0.065(0.001)	0.068(0.004)	0.092(0.014)	0.064(0.001)	0.064(0.005)	0.090(0.003)	0.088(0.007)	0.011(0.001)	0.019(0.004)
Tb	0.000	0.000	0.008(0.002)	0.000	0.000	0.000	0.000	0.000	0.000
Dy	0.024(0.001)	0.023(0.001)	0.037(0.007)	0.032(0.004)	0.030(0.002)	0.042(0.003)	0.039(0.001)	0.000	0.000
Er	0.000	0.000	0.008(0.002)	0.000	0.000	0.000	0.000	0.000	0.000
Tm	0.000	0.000	0.008(0.001)	0.007(0.001)	0.008(0.001)	0.000	0.000	0.000	0.000
Yb	0.000	0.000	0.000	0.000	0.000	0.000	0.000	0.000	0.000
Th	0.059(0.001)	0.033(0.002)	0.040(0.008)	0.042(0.002)	0.031(0.003)	0.041(0.004)	0.024(0.001)	0.007(0.002)	0.027(0.003)
Na	0.000	0.000	0.041(0.008)	0.000	0.000	0.000	0.000	0.000	0.000
K	0.018(0.002)	0.000	0.001(0.001)	0.000	0.000	0.000	0.000	0.000	0.000
Total A	1.606	1.561	1.755	1.830	1.854	1.759	1.774	1.941	1.845

See Figures 1r–v for spot locations. * According to the definition used by Pan & Fleet (1991), allanite requires at least 50% occupancy of the *A*2 site by total rare-earth elements (REE), corresponding to 15 wt%. Therefore, the data on the sample from Kaho in column 1* pertain to REE-rich epidote. *n*: number of microprobe points. Number in parentheses is standard deviation. The compositions are first reported in wt%, then the proportion of cations is reported in atoms per formula unit (*apfu*).

coexist in single crystals implies a distinction in the mechanism responsible for these variants. Compared with the previous EPMA data of allanite in granitic rocks from continental margins and intracontinental settings (*e.g.*, Peterson & MacFarlane 1993, Broska *et al.* 2000, Catlos *et al.* 2000, Wood & Ricketts 2000, Claeson 2002, Kartashov *et al.* 2002, Smith *et al.* 2002, Oberli *et al.* 2004), we contend that Mn-rich allanite is characteristic of such rocks from Japan, except for allanite in granitic (Ovchinnikov & Tzimbalenko 1948, Hutton 1951) and metamorphic rocks (Pavelescu & Pavelescu 1972). An example of the tectonic setting relevant to this Mn-enrichment may be cited from the demonstration by Thonis & Burns (1975) that plate consumption along subduction zones gives rise to at least three environments potentially associated with

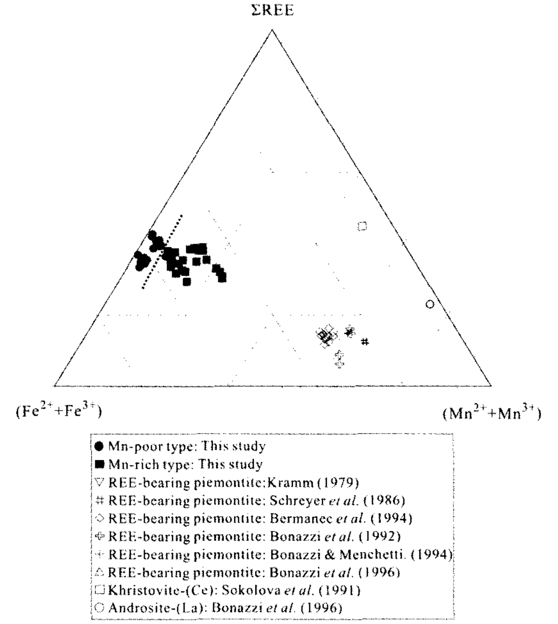

FIG. 2. REE – (Fe^{2+}+Fe^{3+}) – (Mn^{2+}+Mn^{3+}) diagram for Mn-rich epidote-group minerals. The dotted line shows the boundary between Mn-rich and Mn-poor allanite-(Ce), at 0.14 *apfu* Mn. Units are atoms per formula unit (*apfu*).

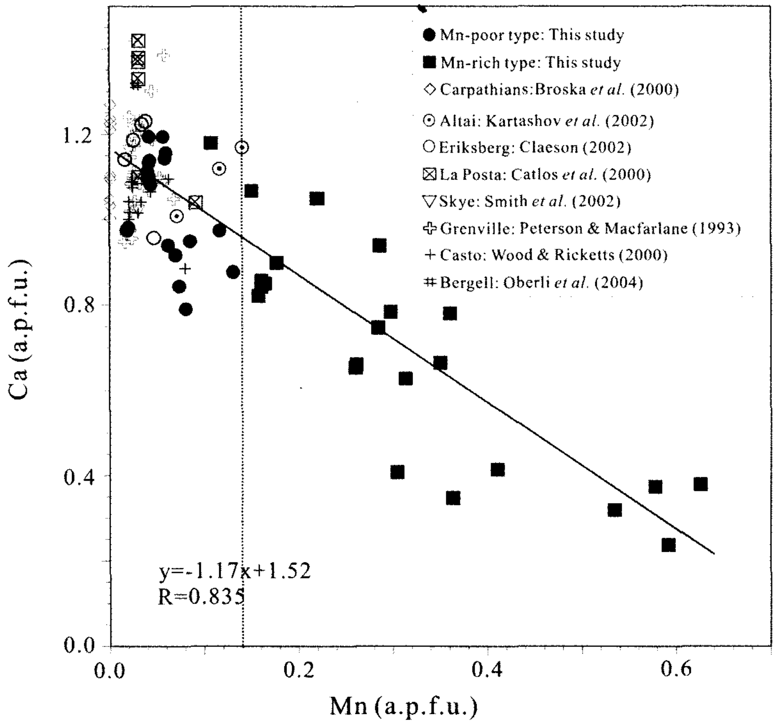

FIG. 3. Plot of Ca *versus* Mn of the allanite-(Ce) samples, suggesting substitution of Mn for Ca. The dashed line shows the boundary between Mn-rich and Mn-poor allanite-(Ce), at 0.14 *apfu* Mn.

production of manganese deposits: 1) manganese mineralization is related to calc-alkaline magmatism, 2) manganese ore deposits are developed in ophiolites, and 3) extensive manganese mineralization exists within the small marine basins located behind island arcs. Moreover, these authors suggested that most of the manganese ore deposits in Japan are formed by the above processes. Accordingly, the present data suggest that one of the far-reaching effects of subduction-zone processes is the formation of Mn-rich allanite as a common constituent of granitic rocks in the Japanese island arc.

The relations between Mn and the REE in allanite from granitic rocks are illustrated in Figures 5–7. Although the REE are not directly related to Mn in allanite from granitic rocks in the intracontinental rifts and continental margins (Figs. 5d–f, 6b, 7b), allanite from granitic rocks in Japan show levels of the REE definitely correlated with Mn (Figs. 5a–c, 6a, 7a). In terms of LREE, Mn varies systematically with La and Nd, whereas Ce exhibits only a small variation (Figs. 5a–c); Mn-rich allanite is marked by low La and high Nd contents. In addition, it is evident from Figure 6a that Mn-rich allanite from granitic rocks invariably contains Y and, to a lesser extent, Sc. Allanite-(Y) in a carbonate vein reported by Peterson & MacFarlane (1993) also incorporates appreciable amounts of Mn (2.35 wt% MnO). The allanite from the Japanese island arc contains significantly more of Y and Sc, in comparison with those from continental margins and intracontinental rifts (Figs. 6a, b). Generally, Y behaves incompatibly in the presence of common silicate minerals, as do MREE to HREE (Best & Christiansen 2001), and Sc is contained in rare HREE-enriched minerals such as thortveitite. In particular, significant amounts of MREE are present in our collection of Mn-rich allanite (Figs. 7a, b). Detailed analysis of the observed variations in REE, Mn and Ca leads to establishment of the coupled substitution:

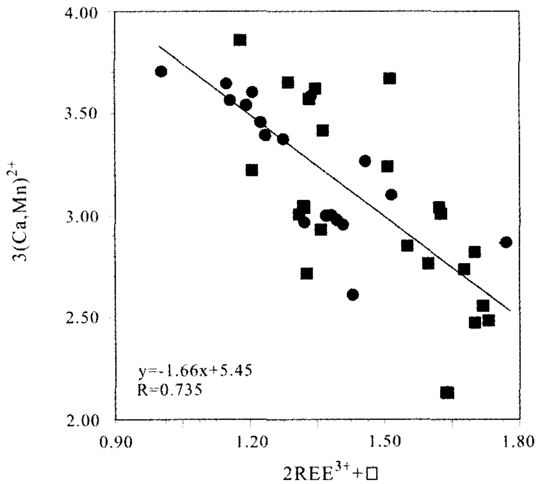

FIG. 4. Plot illustrating the potential coupled substitution at the *A* site of allanite-subgroup minerals from Japan. The substitution plotted is $3(Ca,Mn)^{2+} \rightleftharpoons 2REE^{3+} + \square$, where $\square$ denotes a vacancy at the *A* site. Units: *apfu*; symbols as in Figure 3.

$$Mn^{2+} + (MREE, HREE)^{3+} \rightleftharpoons Ca^{2+} + LREE^{3+}$$

(Mn-rich type) (Mn-poor type)

which is illustrated in Figure 8. This coupled substitution is reported for the first time in allanite.

The REE patterns for the samples examined are consistent with general characteristics of the REE in allanite from igneous rocks (Figs. 9a, b). These patterns indicate that Mn-bearing allanite from granitic rocks could originate from one of two sources. The patterns of Mn-poor allanite of the least fractionated type are distinct from the relatively flat ones of Mn-rich allanite of more fractionated type. The Mn-poor allanite contain high concentrations of the LREE (Fig. 9a), whereas the Mn-rich ones show slight MREE-enrichment (Fig. 9b). Magmatic allanite from the Youngest Toba Tuff (YTT) (Chesner & Ettlinger 1989) and Variscan granitic rocks (Buda & Nagy 1995) have the same patterns, as observed in the Mn-poor samples (Fig. 9a), reflecting enrichment in the LREE. On the other hand, secondary allanite from Torridonian arkoses (Exley 1980) and the rim of allanite from Variscan granitic rocks (Buda & Nagy 1995), influenced by a hydrothermal fluid, have patterns similar to those of the Mn-rich allanite (Fig. 9b). The above characteristics indicate that Mn-rich and Mn-poor samples of allanite-(Ce) have grown from distinct types of granitic melt, both related to subduction-zone activity in the Japanese island arc, but differing in their volatile content. Allanite-subgroup minerals can influence the behavior of not only the LREE but also the MREE and HREE (Y, Sc).

Significance of manganese to the origin and crystallization of allanite-(Ce)

Occurrences of Mn-rich and REE-bearing epidote-group minerals such as androsite-(La) (Bonazzi *et al.* 1996), khristovite-(Ce) (Sokolova *et al.* 1991) and REE-bearing piemontite (Kramm 1979, Schreyer *et al.* 1986, Bermanec *et al.* 1994, Bonazzi *et al.* 1992, 1996, Bonazzi & Menchetti 1994) are located in active continental margins (Innocenti *et al.* 1984, André *et al.* 1986, Wilson 1989). The presence of Mn-rich allanite in the Japanese island arc, in conjunction with the above occurrences, seem to support the hypothesis that Mn-rich epidote-group minerals can be interpreted as one of the far-reaching effects of subduction-zone processes.

Descriptions of manganoan allanite from several localities of Japan by Omori & Hasegawa (1956) and

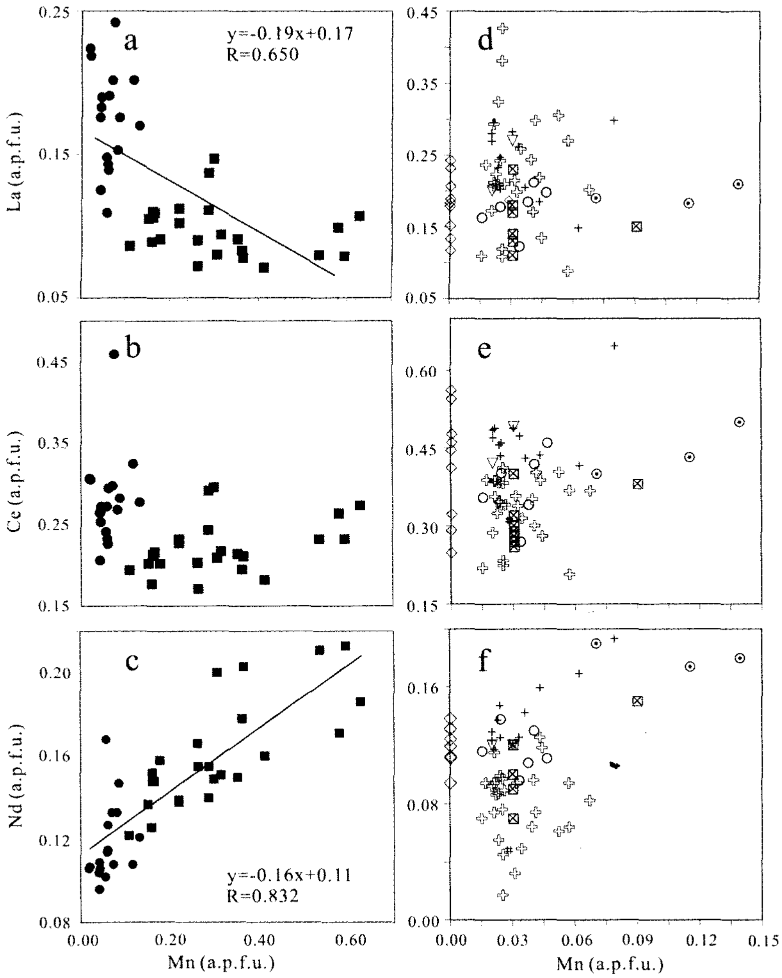

FIG. 5. Compositional variation between Mn and LREE (La, Ce, Nd) for (a–c) the allanite-(Ce) compositions in our suite and (d–f) allanite-subgroup minerals from intracontinental settings and continental margins. Symbols are the same as in Figure 3.

Hasegawa (1957, 1958, 1959, 1960, 1961) illustrate a distinct relation between Mn content and crystal size: manganoan allanite containing more than 5 wt.% MnO closely approximate sizes of 5.0 × 5.0 × 8.0 cm from Mitaichi, 10 cm in length from Shiozawa, and 10 cm in length from Ohari. These crystals are appreciably larger than Mn-poor allanite with less than 3 wt.% MnO and 0.5–4.0 cm length. Furthermore, manganoan allanite containing more than 6 wt.% MnO from Yosemite National Park, California, has been reported to attain 45 mm (Hutton 1951). Consequently, we conclude that allanite crystals attain larger sizes under conditions that also favor the incorporation of Mn (Table 2, Fig. 10). A similar effect of manganese has been recognized with crystallization of garnet from silicic melts at low pressure (Green 1977), as well as on synthesis of large crystals of Mn-bearing anorthite by heating at 1500°C mixtures of the chemical reagents $Al(OH)_3$, $CaCO_3$, $MnCO_3$ and SiO_2 gel under an N_2 atmosphere (Matsui & Kimata 1997). It appears to be essential for the formation of large crystals that these three examples involve the substitution of Mn for Ca.

The regional character of the granitic rocks containing Mn-bearing allanite in the Japanese island arc, on closer inspection, proves to be significant: the granitic rocks containing Mn-poor allanite belong to the magnetite-series granites, whereas those hosting Mn-rich allanite correspond to the ilmenite series (Ishihara 1977, 1981,

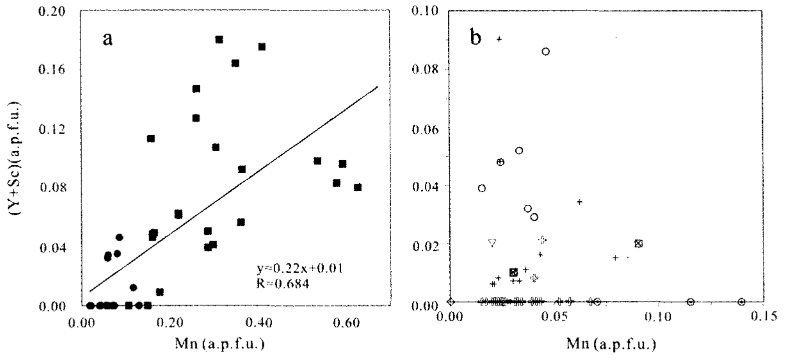

FIG. 6. Plot of (Y + Sc) *versus* Mn for (a) the allanite-(Ce) in our suite and (b) allanite-subgroup minerals from intracontinental settings and continental margins. Symbols are the same as in Figure 3.

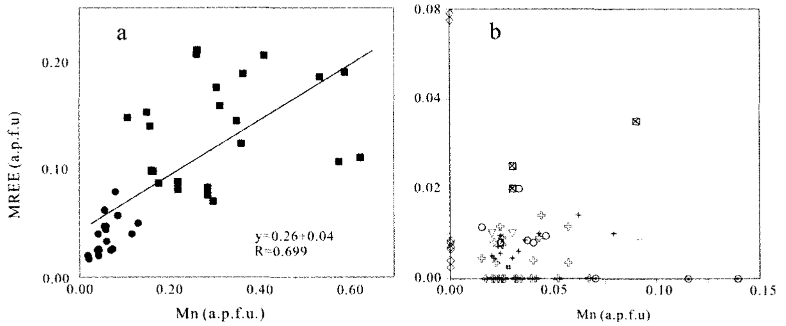

FIG. 7. Plot of MREE (Sm + Gd + Tb + Dy) *versus* Mn for (a) the allanite-(Ce) in our suite and (b) allanite-subgroup minerals from intracontinental settings and continental margins. Symbols are the same as in Figure 3.

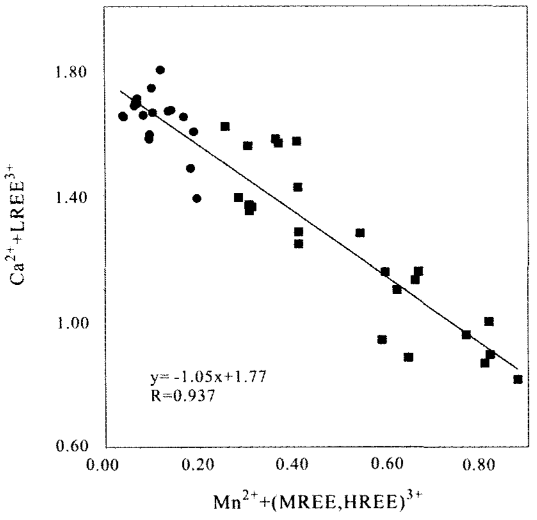

FIG. 8. Plots illustrating a potential coupled substitution between Mn-rich and Mn-poor allanite-(Ce) from granitic rocks, Japan. In all cases, LREE represents the total of La, Ce, Pr and Nd, and MREE = Σ(Sm, Gd, Tb and Dy). HREE represents the sum of Y, Sc, Er, Tm and Yb. Symbols are the same as in Figure 3. Units: *apfu*.

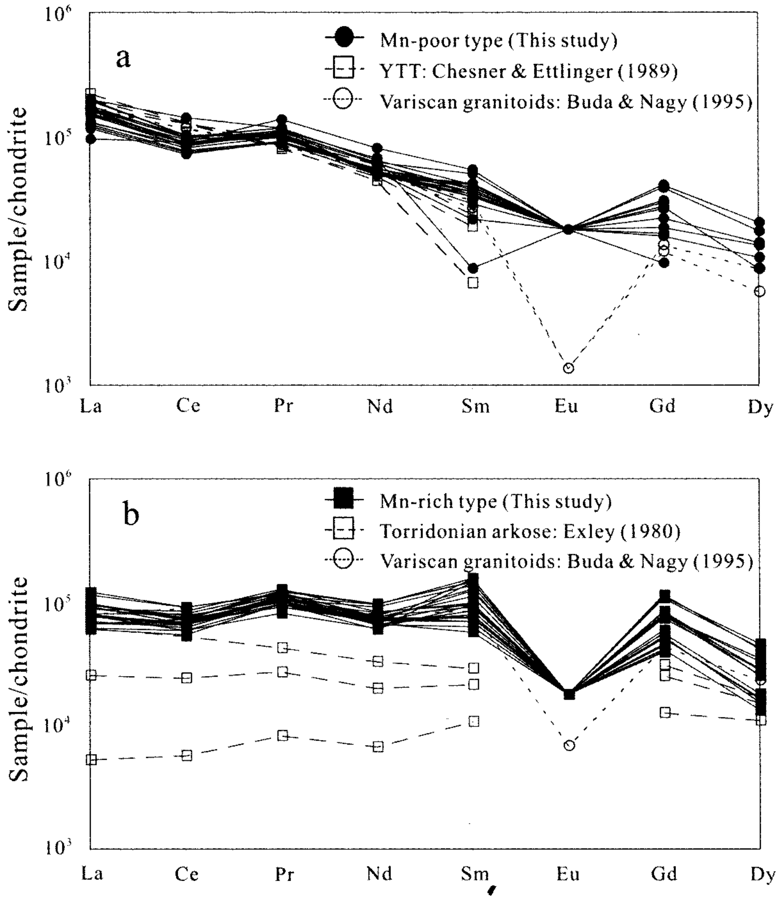

FIG. 9. Plots of chondrite-normalized REE concentrations (as determined by electron-microprobe analysis). Chondrite-normalizing values are taken from Wakita *et al.* (1971). (a) Mn-poor allanite-(Ce) (this study) and allanite-subgroup mineral from the Youngest Toba Tuff (YTT), Sumatra (Chesner & Ettlinger 1989) and Variscan granitic rocks, Hungary (Buda & Nagy 1995), and (b) Mn-rich allanite-(Ce) (this study) and allanite-subgroup minerals from Torridonian arkoses, Skye (Exley 1980), and Variscan granitic rocks, Hungary (Buda & Nagy 1995).

Shibata & Ishihara 1979, Takagi 2004). According to Ishihara's two-fold classification of granitic rocks in the Japanese island arc, affiliation with the ilmenite series implies the crystallization of allanite from a relatively reduced granitic magma under low $f(O_2)$ conditions, whereas the magnetite series implies relatively high $f(O_2)$ conditions. According to Petrík *et al.* (1995), igneous allanite seems to have $Fe^{3+}/(Fe^{3+} + Fe^{2+})$ buffered at about 0.4, whereas vein-type allanite is variably oxidized, and metamorphic allanite can be either oxidized or reduced. Moreover, the magnetite-series granitic rocks are considered to have been generated at greater depth (upper mantle and lowest crust) and not to have interacted with carbonaceous materials. On the other hand, the magma that gave rise to the ilmenite-series granitic rocks was generated in the middle to lower continental crust and mixed with carbonaceous metamorphic and sedimentary rocks at various stages in its igneous history (Ishihara 1977), influenced by H_2O (and lesser amounts of CO_2) residing in minerals and pore spaces.

The I- and S-type granites of Chappell & White (1974) correspond in a very approximate way to granites of the magnetite and the ilmenite series, respectively (Ishihara 1981, Whalen & Chappell 1988). Moreover, although Buda & Nagy (1995) did not directly focus on chemical characteristics of allanite from I- and S-type granitic rocks, they did determine chemical composi-

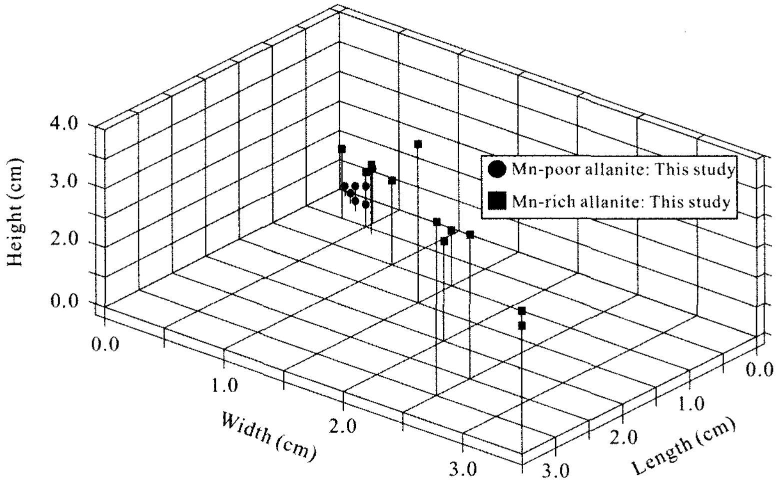

FIG. 10. Crystal size for the Mn-bearing allanite-(Ce) in our suite. Crystals of Mn-rich allanite are larger than the Mn-poor ones.

tions of some REE-bearing accessory minerals in the older and younger Variscan granitic rocks of Hungary. The older rocks are of a syncollision S- or I-type, and migmatitic, associated with a monzonitic suite, whereas the younger rocks consist of post-collision S- or A-type suites associated with granodiorite. Allanite in the older rocks is rich in LREE, whereas those in the younger suite show a slight decrease in LREE and an enrichment in the HREE and Y.

According to White (2001), such magmas fractionate by removal of restite, which causes an increase in the H_2O content, especially in S-type suites. Chappell *et al.* (2004) have proposed that I-type granites can be assigned to low- and high-temperature groups, whereas S-type granitic magmas are apparently of a low-temperature origin. From these studies, it is reasonable to consider that S-type granites may be enriched in H_2O and other volatile components. Accordingly, our suite of Mn-rich allanite-(Ce), derived from the ilmenite-series granitic rocks, can be regarded as a product of a lower-temperature magma enriched in H_2O. The proposal that Mn content in allanite-(Ce) is an indicator of the origin of the host granitic rocks requires further testing.

ACKNOWLEDGEMENTS

We thank Y. Yabe and E. Hashimoto for providing samples from Shiodaira and Kitadosawa, respectively. The authors are indebted to Dr. A. Kyono (University of Tsukuba) for access to the analytical facilities. This manuscript was significantly improved by the reviews of Reto Gieré, an anonymous reviewer and Associate Editor David R. Lentz. This work was funded by a grant from Research Fellowships of the Japan Society for the Promotion of Science for Young Scientists.

REFERENCES

ANDRÉ, L., HERTOGEN, J. & DEUTSCH, S. (1986): Ordovician–Silurian magmatic provinces in Belgium and the Caledonian orogeny in middle Europe. *Geology* **14**, 879-882.

BANNO, Y. (1993): Chromian sodic pyroxene, phengite and allanite from the Sanbagawa blueschists in the eastern Kii Peninsula, central Japan. *Mineral. J.* **16**, 306-317.

BERMANEC, V., ARMBRUSTER, T., OBERHÄNSLI, R. & ZEBEC, V. (1994): Crystal chemistry of Pb- and REE-rich piemontite from Nezilovo, Macedonia. *Schweiz. Mineral. Petrogr. Mitt.* **74**, 321-328.

BEST, M.G. & CHRISTIANSEN, E.H. (2001): *Igneous Petrology*. Blackwell Science, New York, N.Y. (37-44).

BONAZZI, P., GARBARINO, C. & MENCHETTI, S. (1992): Crystal chemistry of piemontites: REE-bearing piemontite from Monte Brugiana, Alpi Apuane, Italy. *Eur. J. Mineral.* **4**, 23-33.

BONAZZI, P. & MENCHETTI, S. (1994): Structural variations induced by heat treatment in allanite and REE-bearing piemontite. *Am. Mineral.* **79**, 1176-1184.

BONAZZI, P., MENCHETTI, S. & REINECKE, T. (1996): Solid solution between piemontite and androsite-(La), a new mineral of the epidote group from Andros Island, Greece. *Am. Mineral.* **81**, 735-742.

BROSKA, I., PETRÍK, I. & WILLIAMS, C.T. (2000): Coexisting monazite and allanite in peraluminous granitoids of the Tribeč Mountains, western Carpathians. *Am. Mineral.* **85**, 22-32.

BUDA, G. & NAGY, G. (1995): Some REE-bearing accessory minerals in two types of Variscan granitoids, Hungary. *Geol. Carpathica* **46**, 67-78.

CARCANGIU, G., PALOMBA, M. & TAMANINI, M. (1997): REE-bearing minerals in the albitites of central Sardinia, Italy. *Mineral. Mag.* **61**, 271-283.

CATLOS, E.J., SORENSEN, S.S. & HARRISON, T.M. (2000): Th–Pb ion-microprobe dating of allanite. *Am. Mineral.* **85**, 633-648.

CHAPPELL, B.W. & WHITE, A.J.R. (1974): Two contrasting granite types. *Pacific. Geol.* **8**, 173-174.

CHAPPELL, B.W., WHITE, A.J.R., WILLIAMS, I.S. & WYBORN, D. (2004): Low- and high-temperature granites. *Trans. R. Soc. Edinburgh, Earth Sci.* **95**, 125-140.

CHESNER, C.A. & ETTLINGER, A.D. (1989): Composition of volcanic allanite from the Toba Tuffs, Sumatra, Indonesia. *Am. Mineral.* **74**, 750-758.

CLAESON, D.T. (2002): Stability of REE-bearing minerals in a metaluminous leucotonalite from the Eriksberg gabbro, Transscandinavian Igneous Belt, Sweden. *Neues Jahrb. Mineral., Abh.* **177**, 277-291.

DAHLQUIST, J.A. (2001): REE fractionation by accessory minerals in epidote-bearing metaluminous granitoids from the Sierras Pampeanas, Argentina. *Mineral. Mag.* **65**, 463-475.

DEER, W.A., HOWIE, R.A. & ZUSSMAN, J. (1986): *Rock-Forming Minerals.* **1B**. *Disilicates and Ring Silicates* (2nd ed.). John Wiley & Sons, New York, N.Y. (151-179).

ERCIT, T.S. (2002): The mess that is allanite. *Can. Mineral.* **40**, 1411-1419.

EXLEY, R.A. (1980): Microprobe studies of REE-rich accessory minerals: implications for Skye granite petrogenesis and REE mobility in hydrothermal systems. *Earth Planet. Sci. Lett.* **48**, 97-110.

GAINES, R.V., SKINNER, H.C.W., FOORD, E.E., MASON, B. & ROSENZWEIG, A. (1997): *Dana's New Mineralogy* (8th ed.). John Wiley & Sons, New York, N. Y. (1195-1205).

GIERÉ, R. & SORENSEN, S.S. (2004): Allanite and other REE-rich epidote-group minerals. *In* Epidotes (A. Liebscher & G. Franz, eds.). *Rev. Mineral. Geochem.* **56**, 431-493.

GREEN, T.H. (1977): Garnet in silicic liquids and its possible use as a P–T indicator. *Contrib. Mineral. Petrol.* **65**, 59-67.

HASEGAWA, S. (1957): Chemical studies of allanites and their associated minerals from the pegmatites in the northern part of the Abukuma massif. *Sci. Rept. Tohoku Univ., Third Ser.* **5**, 345-371.

HASEGAWA, S. (1958): Chemical studies of allanites from the new localities in Fukushima and Kagawa prefectures. *Sci. Rept. Tohoku Univ., Third Ser.* **6**, 39-56.

HASEGAWA, S. (1959): Allanites from the pegmatites of several localities in southwestern Japan. *Sci. Rept. Tohoku Univ., Third Ser.* **6**, 209-226.

HASEGAWA, S. (1960): Chemical composition of allanite. *Sci. Rept. Tohoku Univ., Third Ser.* **6**, 331-387.

HASEGAWA, S. (1961): Chemical compositions of allanite, fergusonite and monazite from the Ushiroda pegmatite, Ishikawa town, Fukushima Prefecture. *J. Jap. Assoc. Mineral., Petrol., Econ. Geol.* **46**, 57-61 (in Japanese).

HOSHINO, M., KIMATA, M., NISHIDA, N., KYONO, A., SHIMIZU, M. & TAKIZAWA, S. (2005): The chemistry of allanite from the Daibosatsu Pass, Yamanashi, Japan. *Mineral. Mag.* **69**, 403-423.

HUTTON, C.O. (1951): Allanite from Yosemite National Park, Tuolumne Co., California. *Am. Mineral.* **36**, 233-248.

INNOCENTI, F., KOLIOS, N., MANETTI, P., MAZZUOLI, R., PECCERILLO, G., RITA, F. & VILLARI, L. (1984): Evolution and geodynamic significance of the Tertiary orogenic volcanism in northeastern Greece. *Bull. Volcanol.* **47**, 25-37.

ISHIHARA, S. (1977): The magnetite-series and ilmenite-series granitic rocks. *Mining Geol.* **27**, 293-305.

ISHIHARA, S. (1981): The granitoid series and mineralization. *Econ. Geol., 75th Anniv. Vol.*, 458-484.

KARTASHOV, P.M., FERRARIS, G., IVALDI, G., SOKOLOVA, E. & MCCAMMON, C.A. (2002): Ferriallanite-(Ce), $CaCeFe^{3+}AlFe^{2+}(SiO_4)(Si_2O_7)O(OH)$, a new member of the epidote group: description, X-ray and Mössbauer study. *Can. Mineral.* **40**, 1641-1648.

KRAMM, U. (1979): Kanonaite-rich viridines from the Venn–Stavelot Massif, Belgian Ardennes. *Contrib. Mineral. Petrol.* **69**, 387-395.

MATSUI, T. & KIMATA, M. (1997): Crystal chemistry of synthetic Mn-bearing anorthite: incorporation of $MnAl_2Si_2O_8$ end-member into feldspar. *Eur. J. Mineral.* **9**, 333-344.

NAGASHIMA, O. & NAGASHIMA, K. (1960): Allanite. *In* The Rare Earth Minerals of Japan. Chigakukenkyu-Kai, Kyoto, Japan (173-184; in Japanese).

NISHIDA, N., KIMATA, M. & SUGIMOTO, A. (1999): Quantitative electron-probe microanalysis of various kinds of rare-earth elements in minerals. *J. Mineral. Soc. Japan* **28**, 71-81 (in Japanese with English abstr.).

OBERLI, F., MEIER, M., BERGER, A., ROSENBERG, C.L. & GIERÉ, R. (2004): U–Th–Pb and $^{230}Th/^{238}U$ disequilibrium isotope systematics: precise accessory mineral chronology and melt evolution tracing in the Alpine Bergell intrusion. *Geochim. Cosmochim. Acta* **68**, 2543-2560.

OMORI, K. & HASEGAWA, S. (1956): Chemical compositions of perthite, ilmenite, allanite and pyroxmangite occurred in pegmatites of a vicinity of Iwaizumi Town, Iwate Prefecture. *Sci. Rept. Tohoku Univ., Third Ser.* **5**, 129-137.

OVCHINNIKOV, L.N. & TZIMBALENKO, M.N. (1948): Mangan-orthite from Vishnevy Mts. *Dokl. Acad. Sci., USSR* **63**, 191-194 (in Russ.).

PAN, YUANMING & FLEET, M.E. (1991): Vanadian allanite-(La) and vanadian allanite-(Ce) from the Hemlo gold deposit, Ontario, Canada. *Mineral. Mag.* **55**, 497-507.

PAVELESCU, L. & PAVELESCU, M. (1972): Study of some allanites and monazites from the south Carpathians (Romania). *Tschermaks Mineral. Petrogr. Mitt.* **17**, 208-214.

PETERSON, R.C. & MACFARLANE, D.B. (1993): The rare-earth-element chemistry of allanite from the Grenville Province. *Can. Mineral.* **31**, 159-166.

PETRÍK, I., BROSKA, I., LIPKA, J. & SIMAN, P. (1995): Granitoid allanite-(Ce): substitution relations redox conditions and REE distributions (on an example of I-type granitoids, western Carpathians, Slovakia). *Geol. Carpathica* **46**, 79-94.

POITRASSON, F. (2002): In situ investigations of allanite hydrothermal alteration: examples from calc-alkaline and anorogenic granites of Corsica (southeast France). *Contrib. Mineral. Petrol.* **142**, 485-500.

REED, S.J.B. & BUCKLEY, A. (1998): Rare-earth element determination in minerals by electron-probe microanalysis: application of spectrum synthesis. *Mineral. Mag.* **62**, 1-8.

SAKAI, C., HIGASHINO, T. & ENAMI, M. (1984): REE-bearing epidote from Sanbagawa pelitic schists, central Shikoku, Japan. *Geochem. J.* **18**, 45-53.

SCHREYER, W., FRANSOLET, A.M. & ABRAHAM, K. (1986): A miscibility gap in trioctahedral Mn–Mg–Fe chlorites: evidence from the Lienne Valley manganese deposit, Ardennes, Belgium. *Contrib. Mineral. Petrol.* **94**, 333-342.

SHIBATA, K. & ISHIHARA, S. (1979): Initial ^{87}Sr/^{86}Sr ratios of plutonic rocks from Japan. *Contrib. Mineral. Petrol.* **70**, 381-390.

SMITH, M.P., HENDERSON, P. & JEFFRIES, T. (2002): The formation and alteration of allanite in skarn from the Beinn an Dubhaich granite aureole, Skye. *Eur. J. Mineral.* **14**, 471-486.

SOKOLOVA, E.V., NADEZHINA, T.N. & PAUTOV, L.A. (1991): Crystal structure of a new natural silicate of manganese from the epidote group. *Sov. Phys. Crystallogr.* **36**, 172-174.

SORENSEN, S.S. (1991): Petrogenetic significance of zoned allanite in garnet amphibolites from a paleo-subduction zone: Catalina Schist, southern California. *Am. Mineral.* **76**, 589-601.

SUZUKI, K., ADACHI, M. & YAMAMOTO, K. (1990): Possible effects of grain-boundary REE on the REE distribution in felsic melts derived by partial melting. *Geochem. J.* **24**, 57-74.

TAKAGI, T. (2004): Origin of magnetite- and ilmenite-series granitic rocks in the Japan arc. *Am. J. Sci.* **304**, 169-202.

THONIS, M. & BURNS, R.G. (1975): Manganese ore deposits and plate tectonics. *Nature* **253**, 614-616.

WAKITA, H., REY, P. & SCHMITT, R.A. (1971): Abundances of the 14 rare-earth elements and 12 other trace elements in Apollo 12 samples: five igneous and one breccia rocks and four soils. *Proc. Second Lunar Sci. Conf.* **2**, 1319-1329.

WHALEN, J.B. & CHAPPELL, B.W. (1988): Opaque mineralogy and mafic mineral chemistry of I- and S-type granites of the Lachlan fold belt, southeast Australia. *Am. Mineral.* **73**, 281-296.

WHITE, A.J.R. (2001): Water, restite and granite mineralisation. *Aust. J. Earth Sci.* **48**, 551-555.

WILSON, M. (1989): *Igneous Petrogenesis.* Chapman & Hall, London, U.K. (191-225).

WOOD, S.A. & RICKETTS, A. (2000): Allanite-(Ce) from the Eocene Casto granite, Idaho: response to hydrothermal alteration. *Can. Mineral.* **38**, 81-100.

YAMADA, S., OKAMOTO, A., TAKADA, M., FUJIWARA, T. & TAKEMURA, M. (1980): On the thortveitite, fluocerite, pyroxferroite and other minerals from the Isanago mine, Ōro, Nakagun Kyoto Prefecture. *Chigaku Kenkyu* **31**, 205-222 (in Japanese).

Received January 17, 2005, revised manuscript accepted December 5, 2005.